Dermal macrophages set pain sensitivity by modulating tissue NGF levels through SNX25–Nrf2 signaling

Tatsuhide Tanaka (ttanaka@naramed-u.ac.jp)
Nara Medical University
Hiroaki Okuda
Kanazawa University
Yuki Terada
Nara Medical University
Ayami Isonishi
Nara Medical University
Masahiro Kitabatake
Nara Medical University
Takeaki Shinjo
Nara Medical University
Kazuya Nishimura
Nara Medical University
Shoko Takemura
Nara Medical University
Hidemasa Furue
Hyogo College of Medicine
Kouko Tatsumi
Nara Medical University
Akio Wanaka
Nara Medical University

Article

Keywords: Dermal macrophage, Pain sensing, SNX25, NGF, Nrf2

Posted Date: September 8th, 2021

DOI: https://doi.org/10.21203/rs.3.rs-869917/v1

Version of Record: A version of this preprint was published at Nature Immunology on January 26th, 2023. See the published version at https://doi.org/10.1038/s41590-022-01418-5.

Abstract

Crosstalk between peripheral neurons and immune cells plays important roles in pain sensation. We identified sorting nexin 25 (Snx25) as a pain-modulating gene in a transgenic mouse line with reduced pain behavior. Snx25 conditional-KO (cKO) in monocyte/macrophage-lineage cells but not in the peripheral sensory neurons reduced pain responses in both normal and neuropathic conditions. Cross transplantation experiments of bone marrows between cKO and wild type (WT) mice revealed that cKO macrophages caused dull phenotype in WT mice and WT macrophages in turn increased pain behavior in cKO mice. SNX25 in dermal macrophages enhances NGF (one of the key factors in pain sensation) production by inhibiting ubiquitin-mediated degradation of Nrf2, a transcription factor that activates Ngf mRNA synthesis. We conclude that dermal macrophages set pain sensitivity by producing and secreting NGF into the dermis in addition to their host defense functions.

Introduction

The skin is frequently stressed by mechanical trauma. Sensory stimuli impinging on skin are encoded by peripheral sensory neurons that can be classified into low-threshold mechanoreceptors (LTMRs), which detect innocuous tactile stimuli, and nociceptors, which exclusively respond to harmful stimuli[1, 2]. Dorsal root ganglion (DRG) neurons are highly diverse in terms of cell size, gene expression and myelination level. While small-diameter neurons are the pain-sensing neurons, medium- to large-diameter neurons preferentially detect low-threshold mechanical stimulation[3]. Tissue damage of skin leads to the release of inflammatory mediators by activated nociceptors or by nonneural cells that reside within or infiltrate into the injured area, including macrophages, mast cells, neutrophils, keratinocytes, and fibroblasts. These inflammatory mediators, such as serotonin, histamine, ATP, and nerve growth factor (NGF), act directly on the nociceptors. Although peripheral sensitization after tissue injury is well described in the skin[2], the roles of immune cells under normal conditions or in acute pain sensation are not fully understood. Recent studies have uncovered a close association of macrophages with peripheral neurons; tissue macrophages can be divided into two subsets, namely a nerve-associated and a blood vessel-associated population[4]. A subset of skin macrophages is closely associated with peripheral nerves and promotes their regeneration when damaged[5]. In neuropathic conditions, macrophages can accelerate pain sensation by sensing tissue angiotensin 2[6] or complement 5a[7,8]. In the latter model, macrophages drive a “vicious cycle”: macrophages secrete NGF into tissues and the NGF in turn stimulates macrophages.

NGF is important for generation of pain and in hyperalgesia in diverse pain states[9]. In addition to enhancing the activity of nociceptive ion channels to promote rapid depolarization and sensitization, NGF also mediates changes in gene expression and membrane localization, both of which contribute to increased sensory neuron excitability[9]. In humans, hereditary sensory and autonomic neuropathy type V (HSAN V) (OMIM 608654), characterized by a marked absence of pain sensibility, is caused by mutations in the *Ngf* gene[10]. Mouse models for HSAN V have been generated, in which the biological activity of NGF

is blocked either by neutralizing antibodies[11] or by *Ngf* expression being abolished with homologous recombination[12]. These mice show a significant reduction of sensory innervations, which leads to decreased pain perception[13]. Collectively, these studies show that NGF is expressed in immune cells including macrophages and facilitates pain transmission by sensory neurons through a variety of mechanisms. Although the level of NGF should be maintained within an optimal range for sensing the normal environment and for evading noxious pain sensation, the mechanisms underlying its regulation remain to be determined.

We serendipitously discovered a pain-insensitive transgenic mouse line. Forward genetic analyses of the mouse led us to identify *sorting nexin 25* (*Snx25*) as a pain-modulating gene. SNX family members are involved in membrane trafficking, cell signaling, membrane remodeling, and organelle motility[14]. We demonstrate here that SNX25 in dermal macrophages activates NGF production by inhibiting ubiquitin-mediated degradation of Nrf2, one of the key transcription factors that activates *Ngf* mRNA transcription[15]. SNX25 in dermal macrophages modulates acute pain sensing under both normal and painful conditions via NGF/TrkA signaling. These findings indicate that macrophage-to-neuron signaling is important in pain processing even in naïve skin in addition to in neuropathic or inflammatory situations.

Results

Snx25+/- mice show a pain-insensitive phenotype

We serendipitously found that pain responses to mechanical stimuli were reduced in Tg (Mlc1-tTA) #Rhn mice (strain name, B6; CBB6(129)-Tg (Mlc1-tTA) 2Rhn) during handling and genotyping of the mice[16] (**Fig. 1a**). The TG mouse was on a mixed genetic background of the 129S6, CBA, and C57BL/6J strains. To negate the possibility that the pain-insensitive phenotype was derived from the mixed genetic background, we back-crossed the TG mice with C57BL/6J mice for seven generations to obtain a genetic background indistinguishable from that of wild type (WT) C57BL/6J mice. Even with the same genetic background, the pain response to mechanical stimuli was also reduced in the TG mice (**Fig. 1b**). Notably, the TG mice were insensitive to mechanical stimuli in normal conditions without any neuropathic or inflammatory paradigm (**Fig. 1a-b**). We also noticed that pain responses to a chemical stimulus, such as lifting, shaking, and licking of the paw, were significantly reduced in the TG mice (**Fig. 1c-d**). Immunohistochemistry revealed that the number of c-Fos-positive cells in the spinal dorsal horn after 5% formalin injection into hind paw skin was lower in TG than in WT mice (**Extended Data Fig. 1a-b**). Since the TG mouse harbors a BAC transgene (clone RP23-114I6, 198kb), we first speculated that an exogenous gene(s) in the BAC might modulate pain behavior. Using next-generation sequencing (NGS), we determined the genome insertion site of the BAC transgene (83 kb out of 198 kb) into 8qB1.1 of chromosome 8 in the TG mouse (**Extended Data Fig. 1c**). The expression levels of exogenous BAC-borne *Mlc1*and *Mov10l1*, however, were indistinguishable from those in WT mice (**Extended Data Fig. 1c–e**). We next hypothesized that the transgene might affect endogenous gene expression and thereby influence

pain behavior. NGS analyses also revealed that the transgene (83kb) was inserted in the 8qB1.1 region, resulting in deletion of three genes (*Snx25*, *Slc25a4*, and *Cfap97*) (**Extended Data Fig. 1c**). Subsequent cDNA microarray analyses confirmed that these endogenous gene expressions were almost null (**Extended Data Fig. 1f**). One or a combination of these gene knockouts could be responsible for the pain behavior. We focused on *Snx25* (**Extended Data Fig. 1g-h**) and obtained commercially available *Snx25* knockout (KO) mice (see Methods) and checked pain behavior of the KO mice. The KO construct was a KO-first conditional allele targeting vector allowing expression monitoring[17]. In the targeting construct, an *En2SA*-IRES-*lacZ* cassette was inserted upstream of exon 4 of *Snx25*, to create a null allele by splicing and premature termination of the transcript (**Fig. 2a**). SNX25 is widely expressed in different tissues with a particular abundance in the lung[18]. *Snx25* -/- mice are embryonic lethal, and therefore we first measured SNX25 expression in the lung of heterozygotes. SNX25 expression in the *Snx25* +/- mouse was approximately half of that in the WT mouse (**Fig. 2b**). The pain responses to mechanical (**Fig. 2c**) and chemical stimuli (**Fig. 2d-e**) were reduced in *Snx25* +/- mice to levels comparable to those in *Mlc*1 TG mice. Although thermal nociception in the *Snx25* +/- mice was not affected at 2 months of age, older mice of 6-8 months-old displayed a higher latency to respond to a heat stimulus (**Extended Data Fig. 2a**). To further determine whether the *Snx25* +/- mice show a dull phenotype after nerve injury, we assessed mechanical hypersensitivity induced by spared nerve injury (SNI). The responses of the *Snx25* +/- mice were significantly attenuated as compared to the WT mice after SNI (**Fig. 2f**). These results indicate that pain responses were reduced not only under normal conditions but also under painful conditions in the *Snx25* +/- mice. We checked cellular size distribution (**Extended Data Fig. 2b**) and the expression of small (CGRP) (**Extended Data Fig. 2c**) and large (NF200) (**Extended Data Fig. 2d**) neuron markers in the DRG of the *Snx25* +/- mice. These data revealed that the sensory neurons of the heterozygotes were indistinguishable from those of the WT mice, indicating that abnormal reactions to pain stimuli were not the result of the loss of neuronal subsets.

Pain-related factors are reduced in *Snx25* +/- mice

To further investigate the roles of SNX25 in pain sensation, we examined the expression of pain-related factors. Consistent with the pain-insensitive phenotype, the expression of pain-related factors including TRPV1 and TrkA was down-regulated in the DRG (**Fig. 2g-k**), sciatic nerve, and spinal cord of *Snx25* +/- mice (**Extended Data Fig. 2e-f**). Capsaicin is a well characterized compound that produces a sensation of pain and stimulates TRPV1 channels on peripheral sensory nerves. Capsaicin elevated the intracellular Ca level in a population of primary cultured DRG neurons, but the amplitude of this Ca elevation was significantly lower in *Snx25* +/- neurons than in WT neurons, indicating that SNX25 deficiency resulted in TRPV1 channel inactivation in the DRG neurons (**Fig. 2l**). We also observed that the mRNA levels of *Trpv1*, *Scn9a*, and *Scn10a*, which are related to pain perception[9], were reduced in *Snx25* +/- DRGs (**Fig. 2m**). From these data, we conclude that the pain-insensitive phenotype of the *Snx25*+/- mice was due to reduced levels of pain-related factors in the peripheral sensory neurons.

DRG-specific *Snx25* cKO mice do not show pain-insensitive phenotype

To further define the tissues and cells responsible for the pain-insensitive phenotype in *Snx25*+/- mice, conditional alleles were generated by removal of the gene-trap cassette by Flippase (FLP), which reverts the mutation to wild type (WT), leaving *loxP* sites on either side of the critical exon 4[17] (**Extended Data Fig. 3a**). We found that pain responses to mechanical (**Extended Data Fig. 3b**) and chemical stimuli (**Extended Data Fig. 3c**) reverted to the normal level in $Snx25^{loxP/loxP}$ mice, underlining the idea that the pain-insensitive phenotype was due to the lack of the *Snx25* gene. To further assess the role of SNX25 in pain behavior, we next conditionally knocked out *Snx25* in the DRG by crossing $Snx25^{loxP/loxP}$ mice with *Advillin* (*Avil*)$^{Cre\text{ERT2}}$ mice[19]. We administered 0.05% tamoxifen (TAM) orally for 2 weeks (**Extended Data Fig. 3d**), a method that is convenient for continuous administration and results in efficient induction of recombination while minimizing stress on the mice[20]. Continuous feeding with TAM-containing chow markedly reduced expression of SNX25 in the DRG (**Extended Data Fig. 3e**). Contrary to our expectation, $Avil^{Cre\text{ERT2/WT}}$; $Snx25^{loxP/loxP}$ mice had normal pain responses to both mechanical and chemical stimuli (**Extended Data Fig. 3f–h**). We also observed that the mRNA levels of *Trpv1*, *Scn9a*, and *Scn10a* were not reduced in DRGs of $Avil^{Cre\text{ERT2/WT}}$; $Snx25^{loxP/loxP}$ mice (**Extended Data Fig. 3i**). These results indicate that SNX25 in the DRG neither regulates pain-related factors nor affects pain sensation. Another possibility is that SNX25 deficiency might reduce sprouting and/or arborization of peripheral sensory fibers. To test the possibility, we compared the PGP9.5-immunoreactive sensory fibers in the dermis of WT and SNX25 +/- mice. The area of PGP9.5-immunoreactive fibers in the hind paw skin of *Snx25* +/- mice were comparable to that of WT mice at 2 months of age (**Extended Data Fig. 3j-k**). These results indicate that the dull phenotype in the *Snx25*+/- mice is not due to reduced skin innervation.

SNX25 in BM-derived macrophages contributes to pain sensation

Given that the DRG cKO showed normal pain behavior, we next focused on immune cells, since *Snx25* +/- mice showed the pain-insensitive phenotype in an acute inflammatory pain model (**Fig. 2d-e**). Among immune cells in the skin, a subset of macrophages in the dermis are associated with peripheral nerves[4], and are therefore good candidates for pain-regulating cells. We confirmed that a population of dermal macrophages (positive for MHCII, CD206, or F4/80) were closely associated with PGP9.5-positive sensory fibers and were SNX25-immunoreactive (**Fig. 3a**, **Extended Data Fig. 4a**). We first checked whether SNX25 in these macrophages could influence migration from bone marrow to dermis. Immunohistochemistry revealed that the numbers of CD206- or MHCII-positive macrophages in hind paw skin of *Snx25* +/- mice were comparable to those in the WT mice (**Extended Data Fig. 4b**). The expression level of CD206 in hind paw skin of *Snx25* +/- mice was also similar to that of WT mice (**Extended Data Fig. 4c-d**). We also analyzed the ultrastructure of the primary cultured macrophages using transmission electron microscopy. There was no significant difference in overall morphology and subcellular organelles between WT- and *Snx25* +/- mice-derived macrophages (**Extended Data Fig. 4e**). These results indicate that the pain-insensitive phenotype in the *Snx25*+/- mice is not due to reduced number nor to abnormal morphologies of dermal macrophages.

Unlike tissue-resident macrophages (e.g., microglia in the brain and Kupffer cells in the liver), dermal macrophages in the skin have been shown to be partly derived from bone marrow (BM) and to turn over[5,21,22]. To confirm these features, we transplanted BM from GFP mice (C57BL/6-Tg (CAG-EGFP)) into WT mice that were pre-treated with busulfan, which is an efficient reagent to suppress bone marrow cells[23]. We confirmed that 78% of myeloid blood cells were of donor origin at 10 weeks after BM transplantation (**Fig. 3b–c, Extended Data Fig. 5a**) and that donor-derived dermal macrophages expressed MHCII, CD206, F4/80, Lyve1 (**Fig. 3d, Extended Data Fig. 5b–d**) and *Cx3cr1* (**Fig. 3e**). GFP-positive cells were predominant in MHCII-expressing macrophages (**Extended Data Fig. 5e–f**). In contrast, only a few GFP-positive neutrophils (Gr1), B-cells (CD19), killer T-cells (CD8a), helper T-cells (CD4) and NK cells (NK1.1) were detected in hind paw skin (**Extended Data Fig. 5g-k**). GFP-positive cells were not found in the gray matter of the spinal dorsal horn (**Extended Data Fig. 5l**). Consistent with previous reports[24], these results indicate that spinal cord microglia are not derived from BM in adult. To gain further insight into the contribution of dermal macrophages to pain sensation, we made BM chimeric mice by cross-transplanting WT and *Snx25* +/- BMs (**Fig. 3f**). Interestingly, the 50% withdrawal threshold to mechanical stimuli in the paws increased in the WT mice with *Snx25* +/- BM transplant and, in turn, decreased in the *Snx25* +/- mice with WT BM transplant (**Fig. 3g**). Mice treated with busulfan but not with BM transplantation exhibited normal withdrawal thresholds (data not shown). BM transplantation between the same genotypes (WT or SNX25 +/-) did not change mechanical sensitivities (data not shown). Taken altogether, SNX25 in BM-derived immune cells including dermal macrophages, but not spinal microglia, likely contributes to pain sensation.

The number of macrophages in hind paw skin in *Snx25* +/- mice was normal (**Extended Data Fig. 4b**). However, given that the pain response to a chemical stimulus as an acute inflammatory pain model was extremely reduced in *Snx25* +/- mice (**Fig. 2d-e**), we next sought to determine the function of macrophages in the inflammatory environment. Immunohistochemistry revealed that the accumulation of macrophages after formalin injection was reduced in *Snx25* +/- mice (**Extended Data Fig. 6a**). We also found that at 3 d after formalin injection, the expression of a cluster of chemokines was lower in *Snx25* +/- mice than in WT mice (**Extended Data Fig. 6b**). Low macrophage accumulation in *Snx25* +/- mice may be due to this reduction of chemokine expression. These immune phenotypes may be attributable to upregulation of TGF-beta receptor-1 (**Extended Data Fig. 6c**), which is known to suppress immune responses[25] and to be degraded by SNX25[18]. From these data, we conclude that the abnormality in function of dermal macrophages in *Snx25* +/- mice affects pain sensation under normal and inflammatory conditions.

Snx25 conditional KO in macrophages yields a pain-insensitive phenotype

To further target the dermal macrophages, we generated mice having *Snx25* cKO in the monocyte/macrophage lineage by crossing $Snx25^{loxP/loxP}$ mice with $Cx3cr1^{Cre\text{ERT2/WT}}$ mice[26]. As expected, $Cx3cr1^{Cre\text{ERT2/WT}}$; $Snx25^{loxP/loxP}$ mice exhibited reduced pain responses to mechanical (**Fig. 4a–b**) and chemical stimuli (**Fig. 4c**). Size distribution and the expression of small or large neuron markers in

the DRG were normal in *Cx3cr1*^{Cre}ERT2/WT; *Snx25*$^{loxP/loxP}$ mice, indicating that abnormal reactions to pain were not the result of the loss of a particular neuron type (data not shown). However, the mRNA levels of *Scn9a* and *Scn10a* were reduced in the DRG of *Cx3cr1*^{Cre}ERT2/WT; *Snx25*$^{loxP/loxP}$ mice (**Fig. 4d**). Consistent with the results in *Snx25* +/- mice, the expression of chemokines and cytokines was lower in hind paw skin of *Cx3cr1*^{Cre}ERT2/WT; *Snx25*$^{loxP/loxP}$ mice than in *Snx25*$^{loxP/loxP}$ mice (**Fig. 4e**, **Extended Data Fig. 6d**). To further investigate whether the decrease in chemokine expression really occurs in dermal macrophages, macrophages were selectively collected from the skin of the *Snx25* cKO mice by fluorescence activated cell sorting (FACS) and gene expression patterns were examined. (**Extended Data Fig. 6e-f**). SNX25 depletion in macrophages did decrease the expression of chemokines (**Extended Data Fig. 6g**). These results indicate that SNX25 contributes to the inflammatory response in dermal macrophages of skin after chemical stimuli, as well as to pain sensation under normal conditions.

A recent study demonstrated that Lyve1^{lo}MHCII^{hi}Cx3cr1^{hi} macrophages colocalize with peripheral nerves[4]. To determine the relationship between SNX25-positive dermal macrophages and peripheral nerves, we crossed *Cx3cr1*^{Cre}ERT2/WT; *Snx25*$^{loxP/loxP}$ mice with reporter mice harboring RCL-eNpHR3.0-EYFP (Ai39)[27] (**Fig. 4f**). TAM administration resulted in YFP expression in Cx3cr1/MHCII-positive macrophages (**Fig. 4g**), but not in CD117-positive mast cells (data not shown). YFP-positive dermal macrophages were apposed to PGP9.5-positive fibers in the dermis (**Fig. 4h**), suggesting that SNX25-positive dermal macrophages are closely associated with peripheral sensory fibers.

CX3CR1 is the fractalkine receptor and is found not only on the surface of macrophages but also on the surface of microglia in the central nervous system[28]. Microglia also regulate neuronal and synaptic activities to change pain behavior[29], implying that the pain-insensitive phenotype in the *Cx3cr1*^{Cre}ERT2/WT; *Snx25*$^{loxP/loxP}$ mice could be derived from a microglial abnormality rather than from dermal macrophage dysfunction. To distinguish between the cells responsible (dermal macrophages or microglia) in the *Cx3cr1-Cre* driven *Snx25* cKO mice, we again transplanted BM of *Cx3cr1*^{Cre}ERT2/WT; *Snx25*$^{loxP/loxP}$ mice into *Snx25*$^{loxP/loxP}$ mice (**Fig. 4i**). In these BM chimeric mice, *Snx25* cKO was limited to dermal macrophages; we confirmed that BM-derived cells did not contribute to the microglia in the spinal cord (**Extended Data Fig. 5l**). This finding is consistent with an *in vivo* lineage-tracing study demonstrating that adult microglia are derived from primitive myeloid progenitors before embryonic day 8[24]. Notably, the withdrawal threshold to mechanical stimuli was significantly increased in the *Snx25*$^{loxP/loxP}$ mice having *Cx3cr1*^{Cre}ERT2/WT; *Snx25*$^{loxP/loxP}$ mice's BM transplanted and TAM administered at 35 d after transplantation (**Fig. 4k**), while the same experimental condition without TAM treatment yielded a threshold comparable to the control (before BM transplantation, **Fig. 4j**). Furthermore, in SNI paradigms using the same experimental (+TAM) and control (-TAM) mice as above, TAM treatment attenuated mechanical hypersensitivities that were observed in the control group (**Fig. 4l**). These results indicate that SNX25 in dermal macrophages, but not microglia, is required for pain sensation under both normal and painful conditions.

SNX25 in dermal macrophages is required for pain sensation via NGF signaling

We focused on nerve growth factor (NGF) as a critical factor in the pain-insensitive behavior of mice having *Snx25* cKO in dermal macrophages for two reasons: first, NGF plays critical roles in hyperalgesia and its mutation causes painless phenotypes[30,31]; and second, *Trpv1*, *Scn9a*, and *Scn10a*, whose expression was reduced in the *Snx25* +/- DRGs (**Fig. 2m**), are all transcriptionally regulated by peripheral tissue-derived and retrogradely transported NGF[31]. A plausible scenario is that NGF concentration in the dermis is partly maintained by macrophages in WT mice and that decreased NGF impairs macrophage-to-nerve signaling in the *Snx25* heterozygotes and cKO in macrophages. Consistent with this, the NGF expression level of hind paw skin was decreased in the *Snx25* +/- mice (**Fig. 5a**). We also found that the expression level of NGF was lower at 30 min after formalin injection in hind paw skin of *Snx25* +/- mice than WT mice (**Fig. 5b**). NGF was actually expressed in dermal macrophages in hind paw skin (**Fig. 5c**) and its expression level was reduced in BM-derived macrophages (BMDMs) of *Snx25* +/- mice (**Fig. 5d**). We further conducted a nerve ligation assay to assess the cumulative axonal transport rate of TrkA, which is the cognate receptor for NGF, in sciatic nerves[32]. Eight hours after ligation, perfused sciatic nerve tissues were analyzed immunohistochemically. The accumulation of TrkA receptor on the distal side of the nerve ligature was significantly reduced in the *Snx25* +/- nerves (**Fig. 5e**), supporting the notion that a reduction of NGF in the periphery results in diminished retrograde transportation of the NGF–TrkA complex in the *Snx25* +/- DRG. Quantitative RT-PCR showed decreased *Ngf* mRNA in BMDMs from *Snx25* +/- mice (**Fig. 5f**) or in BMDMs with *Snx25* knockdown (KD), indicating that SNX25 modulates *Ngf* production at the mRNA level (**Fig. 5g**).

We next investigated the molecular mechanisms bridging SNX25 to *Ngf* synthesis. A CNC-bZip transcription factor, NF-E2-related factor 2 (Nrf2), regulates *Ngf* mRNA induction in glial cells[15]. Consistent with that report, we found that *Nrf2*-specific siRNA significantly reduced constitutive *Ngf* gene expression in BMDMs (**Fig. 6a**). We hypothesized that SNX25 regulates Nrf2 level and thereby *Ngf* gene expression. Nrf2 level in the cell is known to be regulated by continuous ubiquitination and proteasome degradation, which is blocked by Keap1 protein[33]. The level of poly-ubiquitinated Nrf2 protein was increased following treatment with a proteasome inhibitor, MG132 (**Fig. 6b**, arrowhead) and was further elevated by siRNA-mediated knockdown of *Snx25* in 293T cells (**Fig. 6c**, arrowheads). *Snx25* overexpression (cells transiently co-transfected with mouse *Snx25* and mouse *Nrf2* expression vectors), in turn, decreased poly-ubiquitinated Nrf2 level compared to empty vector (cells transiently co-transfected with empty vector and mouse *Nrf2* expression vector) in 293T cells (**Fig. 6d**, arrowhead). The soluble-type tamoxifen derivative 4-OH tamoxifen (4-OHT) conditionally decreased *Snx25* in $Cx3cr1^{Cre\text{ERT2/WT}}$; $Snx25^{loxP/loxP}$ BMDMs, and this *in vitro* cKO recapitulated the above-demonstrated increase of poly-ubiquitinated Nrf2 (**Fig. 6e**, arrowhead). SNX16, a member of SNX superfamily, directly binds to eukaryotic translation elongation factor 1A2 and thereby inhibits ubiquitination and degradation of the elongation factor 1A2[34]. To test whether SNX25 regulates ubiquitination of Nrf2 in the same fashion, we performed co-immunoprecipitation (Co-IP) experiments using anti-Nrf2 antibodies in 293T cells (cells transiently co-transfected with mouse *Snx25* and mouse *Nrf2* expression vectors) and confirmed that SNX25 binds to Nrf2 (**Fig. 6f**). *in vitro* ubiquitination assay in BMDM showed an increase in the level of ubiquitinated Nrf2 protein in SNX25-knockdown cells (**Fig. 6g**). Taken together, SNX25-Nrf2 physical

interaction can inhibit the ubiquitination and subsequent degradation of Nrf2. Consistent with this mechanism, heme oxygenase-1 (HO-1), a representative target factor of Nrf2, was decreased in hind paw skin of the *Snx25* +/- mice (**Fig. 6h**).

There is a close relationship between mechanical stimulation and tissue NGF production[35]. We hypothesized that the above-demonstrated SNX25-Nrf2 signaling pathway may link mechanical stimuli to NGF synthesis. In order to test this hypothesis, BMDMs were stretched by 12.5% in a stretch chamber and time courses of SNX25 and NGF expressions were examined by Western blotting. As expected, both SNX25 and NGF were simultaneously increased in response to the mechanical stimuli, although these increases did not reach statistical significance (**Fig. 6i-j**).

An important question is whether dermal macrophages are sufficient to initiate pain sensation without both neuropathic intervention and inflammation. To address this, we depleted dermal macrophages by intradermal injection (i.d.) of clodronate liposomes (Clo-lipo), a well-characterized macrophage killer[36], twice into one side of the hind paw (**Fig. 7a-b**). Immunohistochemistry revealed that the numbers of CD206- or MHCII-positive macrophages were decreased at 3 days after the second Clo-lipo injection relative to the control liposome-injected skin (**Fig. 7c**). Notably, macrophage depletion increased withdrawal thresholds to mechanical stimuli (**Fig. 7e**), while control liposomes did not (**Fig. 7d**). Western blot analyses revealed that NGF, SNX25, and CD206 expression levels were decreased in the Clo-lipo-injected area than in the control liposome-injected area (**Fig. 7f–i**). Taken together, these findings indicate that SNX25 and NGF in dermal macrophages are required for pain sensation under normal conditions.

To further substantiate the importance of SNX25 in pain sensation, we administered 4-OHT by intradermal injection daily for seven days into *Cx3cr1*$^{Cre\text{ERT2/WT}}$; *Snx25*$^{loxP/loxP}$ mice (**Fig. 7j**). At 8 days after the last injection, the 4-OHT-injected hind paw showed a pain-insensitive phenotype, in contrast to the vehicle-injected hind paw (**Fig. 7k**). To visualize cells with recombination by YFP fluorescence, we crossed *Cx3cr1*$^{Cre\text{ERT2/WT}}$; *Snx25*$^{loxP/loxP}$ mice with Ai32; *Snx25*$^{loxP/loxP}$ mice to generate triple TG mice (*Cx3cr1*$^{Cre\text{ERT2/WT}}$; *Snx25*$^{loxP/loxP}$; Ai32/+) (**Fig. 7l**). We injected 4-OHT for seven days (once a day) into the hind paw of the *Cx3cr1*$^{Cre\text{ERT2/WT}}$; *Snx25*$^{loxP/loxP}$; Ai32/+ mice (**Fig. 7l**). YFP expression was detected in macrophages in the 4-OHT-injected hind paw of the triple TG mice, while the vehicle-injected hind paw did not show YFP expression (**Fig. 7m**). Importantly, intradermal injection of 4-OHT did not yield YFP expression in macrophages of the sciatic nerve and the DRG (**Fig. 7m**). The latter finding was of particular interest because recent work has shown that macrophages in the DRG mediate neuropathic pain[37]. The phenotype changes in our BM transplantation experiments **(Fig. 4i-k**) might depend on this DRG macrophages, but not on the dermal macrophages. In support of this hypothesis, BM transplantation experiment using GFP mice (C57BL/6-Tg (CAG-EGFP)) revealed that DRG macrophages were partly derived from bone marrow and to turn over (**Extended Data Fig. 7a-b**), whereas the replacement of macrophages within the sciatic nerve were low (**Extended Data Fig. 7c-d**). To test the contribution of DRG macrophages to pain sensitivity, we administered 4-OHT onto exposed DRGs (L4 and L5) of *Cx3cr1*$^{Cre\text{ERT2/WT}}$; *Snx25*$^{loxP/loxP}$; Ai32/+ mice (**Extended Data Fig. 7e**). At 5 days after

administration, DRGs showed YFP-positive macrophages, while *Snx25*$^{loxP/loxP}$; Ai32/+ mice yielded no YFP expression (**Extended Data Fig. 7f**). At 5 days after administration, ipsilateral hind paws did not show a pain-insensitive phenotype in *Cx3cr1*^{Cre}ERT2/WT; *Snx25*$^{loxP/loxP}$; Ai32/+ mice (**Extended Data Fig. 7g**). These data indicate that SNX25 in dermal macrophages, but not in DRG macrophages, is a pivotal factor for pain sensation under normal conditions.

Collectively, our results indicate that SNX25 activates NGF production by inhibiting ubiquitin-mediated degradation of Nrf2, resulting in increased expression of a number of pain-related genes in the DRG cell bodies (**Fig. 7n**). Based on these data, we conclude that SNX25 in dermal macrophages modulates acute pain sensing under normal and painful conditions.

Discussion

Recent pain research has revealed pain-modulating cells, molecules, and neural pathways, especially in the central nervous system[38]. The functional anatomy[39] and neuro-immune interactions[40] of the peripheral sensory system have been elucidated at remarkable speed in recent years. However, the whole picture of pain-sensing mechanisms remains unclear. In the present study, from a phenotype-driven forward genetic screen of pain-insensitive *Mlc1* TG mice that was free from any specific working hypothesis, we have successfully identified *Snx25* as a pain-modulating gene. Both *Snx25* +/- mice and *Snx25* conditional-KO mice in macrophages displayed reduced pain responses under both normal and painful conditions. SNX25 inhibits the ubiquitination and subsequent proteasome degradation of Nrf2 and thereby maintains NGF production and secretion into tissues. *Snx25* conditional KO, in turn, accelerates Nrf2 degradation and lowers NGF levels, which leads to a dull phenotype (**Fig. 7n**).

Recent progress in gene cataloging techniques such as single-cell RNA sequencing has broadened our knowledge of tissue macrophages. Chakarov et al. characterized two independent populations of lung interstitial macrophages exhibiting distinct gene expression profiles and phenotypes: Lyve1^{lo}MHCII^{hi}Cx3cr1^{hi} macrophages were associated with nerves, whereas Lyve1^{hi}MHCII^{lo}Cx3cr1^{lo} macrophages were preferentially located around blood vessels[4]. These interstitial macrophages were in part derived from bone marrow[4], consistent with fate-mapping studies[5,22]. We confirmed that donor-derived GFP-positive cells also expressed *Cx3cr1* and MHCII in the dermis of recipient mice after BM transplantation (**Fig. 3b–3e**). We crossed *Cx3cr1*^{Cre}ERT2/WT mice with the reporter line, RCL-eNpHR3.0-EYFP (Ai39)[27], and YFP-positive dermal macrophages were frequently found in close proximity to PGP9.5-positive fibers that innervate the skin (**Fig. 4h**). This finding is consistent with a previous report that Cx3cr1^{hi} macrophages colocalize with peripheral nerves, which contributes to the surveillance and regeneration of local nerves in the dermis[5]. NGF production by these dermal macrophages (**Fig. 5c**) likely contributes to the regeneration of local nerves in addition to the maintenance of pain sensibility. Macrophages are known to adhere to the cell matrix at a specialized structure, the podosome[41]. Podosomes confer on dermal macrophages the ability to sense mechanical stress and deformation of tissues[41,42]. It is interesting to speculate that the mechanosensing ability of dermal macrophages is

linked to NGF production and thereby regulates mechanical pain sensitivity. In line with this speculation, SNX25 and NGF were upregulated in response to mechanical stretch in cultured bone marrow-derived macrophages (**Fig. 6i-j**). Notably, *Snx25* +/- mice or *Cx3cr1*^{Cre}ERT2/WT; *Snx25*$^{loxP/loxP}$ mice were insensitive to mechanical stimuli in normal conditions without any neuropathic or inflammatory paradigm (**Fig. 2c, 4b**). Interestingly, our preliminary data revealed that these mice exhibited reduced responses to innocuous low-pressure stimuli[43, 44] (**Extended Data Fig. 8a-b**), suggesting that SNX25 in macrophages might be involved in innocuous tactile sensing in addition to mechanical pain. This aspect is now under investigation.

We showed that SNX25 regulated cellular Nrf2 content by changing its ubiquitination level (**Fig. 6**). Although SNX family members are diverse and are involved in a wide variety of intracellular events such as regulation of vesicle trafficking[14], some of them regulate protein ubiquitination. SNX16 inhibits ubiquitin-mediated proteasomal degradation of eukaryotic translation elongation factor 1A2 in colorectal cancer development[34]. SNX17 recruits USP9X to antagonize ubiquitination and degradation of pericentriolar material 1 during serum starvation-induced ciliogenesis[45]. We also found that *Snx25* knockdown in the macrophage cell line RAW264.7 promoted ubiquitination of IkBa after lipopolysaccharide stimulation[46]. Nrf2 is the principal transcription factor that regulates antioxidant response element-mediated expression of antioxidant enzymes[33]. Recent studies have reported a relationship between Nrf2 and mechanical stimuli[47]. Taking all these observations together, mechanosensory stimuli impinging on skin may stimulate dermal macrophages, and the macrophages then make the NGF concentration optimal for neurons to respond to stimuli via an SNX25–Nrf2 signaling pathway. A recent report showed that IL-23/IL-17A/TRPV1 axis regulates female-specific mechanical pain via macrophage-neuron interactions[48]. The present study has several overlaps (mechanisms originated from macrophages and involvement of TRPV1) with the report, but the SNX25-Nrf2 axis is not female-specific (most of the present data were obtained from male mice), suggesting that both molecular axes may cooperate in mechanical pain sensation.

One of the most important findings in the present study is that lowering NGF levels for a relatively short term yielded mice with the pain-insensitive phenotype in *Snx25* cKO in dermal macrophages (**Fig. 7j-k**) and in mice transplanted with *Snx25* cKO macrophages (**Fig. 4i-l**) in naïve glabrous skin. In human, HSAN V characterized by a marked absence of pain sensibility, is caused by mutations in the *Ngf* gene[10,13]. The NGF suppression by *Snx25* cKO in macrophages mimics HSAN V pathology to some extent, but there is a critical difference between two paradigms: HSAN V is characterized by long-term NGF deficiency and morphological changes in peripheral sensory nerves, such as retraction of nerve endings[49], which we did not see in the *Snx25* cKO dermis (**Extended Data Fig. 3j-k**). A short-term NGF decrease in *Snx25* cKO mice depletes the pain-sensing machinery (Na channels) in DRG neurons (**Fig. 4d**). Based on the clinical phenotypes of HSAN V patients, anti-NGF neutralizing monoclonal antibodies were developed as therapeutic means to mitigate refractory pain[50]. Humanized monoclonal antibodies (tanezumab and fasinumab) have gone to clinical trials with successful pain-relieving effects[51]. Although an unexpected

side effect on joints precluded the monoclonal antibodies to further proceed to bedside, they are still a good target of pain-relieving medicine[51]. The increase of tissue NGF levels, on the other hand, is well characterized in several inflammatory conditions and in several models of pain[52]. Indeed, we showed that the expression level of NGF was elevated at 30 min after formalin injection in hind paw skin (**Fig. 5b**). Taking all these findings into account, we propose that the tissue content of NGF is continuously controlled at least in part by macrophages through SNX25–Nrf2 signaling. In this hypothesis, the tissue levels of NGF parallel the mechanical pain sensitivities: the higher the NGF level, the more sensitive the animal or tissue is, and vice versa. Supporting this hypothesis, a Clo-lipo-mediated purge of dermal macrophages led to lowered NGF levels and concomitant pain-insensitive phenotypes (**Fig. 7d–g**). SNX25–Nrf2 signaling-mediated NGF regulation broadens the role of dermal macrophages. The relationship between macrophages and pain sensation has long been examined and most studies have focused on pathological painful situations[8]. These studies did not check the pain sensitivity in naïve conditions. SNX25–Nrf2 signaling in macrophages has the potential to bridge between the painless phenotype of HSAN V and these hyperalgesia conditions. In due course, it would be tempting to develop small compound(s) that could inhibit the SNX25–Nrf2 signaling pathway. Such compounds may become a promising alternative to the anti-NGF monoclonal antibodies, which have been withheld from clinical applications. We should, however, exercise caution in taking this step; NGF is also produced by noninflammatory cells, such as keratinocytes[53], in addition to other inflammatory cells, such as fibroblasts. Thus, further experiments are needed to determine the entire cellular and molecular mechanism controlling peripheral NGF levels.

Declarations

Acknowledgements

We thank Ms. Mitsuko Banja (Nara Medical University), Dr. Kazunori Sango (Tokyo Metropolitan Institute of Medical Science), Dr. Shenglan Wang (Hyogo University of Health Sciences), Dr. Mariko Yamano (Nara Medical University), Dr. Kazuki Nakahara (Nara Medical University), Dr. Saki Mitani (Osaka Dental University) for technical assistance. We also thank Prof. Masahito Ikawa (Osaka University) and Prof. Toshihiro Ito (Nara Medica l University) for their valuable suggestions and making apparatuses available to us. This work was supported by JSPS KAKENHI JP16K08451 (to HO), JP16K20112 (to YT), JP18K16492 (to TS), JP19K07827 (to TT), JP19K18303 (to YT), JP19K16480 (to AI), the Osaka Medical Research Foundation for Intractable Diseases (to TT), the Takeda Science Foundation (to TT), the Nakatomi Foundation (to TT), the Naito Foundation (to TT), and the Ichiro Kanehara Foundation (to TT).

Author contributions

TT, HO, HF and AW conceived the project and designed the experiments. TT, HO, YT, TS, ST, MK, KN, AI, and KT performed the experiments. TT, HO, MK, AI and KT analyzed the data. TT and AW wrote the paper. AW coordinated and directed the project.

Conflict of Interest Statement

All authors have no affiliations with or involvement in any organization or entity with any financial interest, or non-financial interest in the subject matter or materials discussed in this manuscript.

References

1. Abraira, V. E. & Ginty, D. D. The sensory neurons of touch. *Neuron* **79**, 618–639 (2013).

2. Basbaum, A. I., Bautista, D. M., Scherrer, G. & Julius, D. Cellular and Molecular Mechanisms of Pain. *Cell* **139**, 267–284 (2009).

3. Liu, Y. & Ma, Q. Generation of somatic sensory neuron diversity and implications on sensory coding. *Curr. Opin. Neurobiol.* **21**, 52–60 (2011).

4. Chakarov, S. *et al.* Two distinct interstitial macrophage populations coexist across tissues in specific subtissular niches. *Science* **363**, eaau0964 (2019).

5. Kolter, J. *et al.* A Subset of Skin Macrophages Contributes to the Surveillance and Regeneration of Local Nerves. *Immunity* **50**, 1482-1497.e7 (2019).

6. Shepherd, A. J. *et al.* Angiotensin II triggers peripheral macrophage-to-sensory neuron redox crosstalk to elicit pain. *J. Neurosci.* **38**, 7032–7057 (2018).

7. Shutov, L. P. *et al.* The complement system component C5a produces thermal hyperalgesia via macrophage-to-nociceptor signaling that requires NGF and TRPV1. *J. Neurosci.* **36**, 5055–5070 (2016).

8. Warwick, C. A., Shutov, L. P., Shepherd, A. J., Mohapatra, D. P. & Usachev, Y. M. Mechanisms underlying mechanical sensitization induced by complement C5a: The roles of macrophages, TRPV1, and calcitonin gene-related peptide receptors. *Pain* **160**, 702–711 (2019).

9. Barker, P. A., Mantyh, P., Arendt-Nielsen, L., Viktrup, L. & Tive, L. Nerve growth factor signaling and its contribution to pain. *J. Pain Res.* **13**, 1223–1241 (2020).

10. Einarsdottir, E. *et al.* A mutation in the nerve growth factor beta gene (NGFB) causes loss of pain perception. *Hum. Mol. Genet.* **13**, 799–805 (2004).

11. Ruberti, F. *et al.* Phenotypic knockout of nerve growth factor in adult transgenic mice reveals severe deficits in basal forebrain cholinergic neurons, cell death in the spleen, and skeletal muscle dystrophy. *J. Neurosci.* **20**, 2589–2601 (2000).

12. Chen, K. S. *et al.* Disruption of a single allele of the nerve growth factor gene results in atrophy of basal forebrain cholinergic neurons and memory deficits. *J. Neurosci.* **17**, 7288–7296 (1997).

13. Capsoni, S. From genes to pain: Nerve growth factor and hereditary sensory and autonomic neuropathy type V. *Eur. J. Neurosci.* **39**, 392–400 (2014).

14. Teasdale, R. & Collins, B. Insights into the PX (phox-homology) domain and SNX (sorting nexin) protein families: structures, functions and roles in disease. *Biochem J.* **44**, 39–59 (2012).

15. Mimura, J. *et al.* Nrf2 regulates NGF mRNA induction by carnosic acid in T98G glioblastoma cells and normal human astrocytes. *J. Biochem.* **150**, 209–217 (2011).

16. Tanaka, K. F. *et al.* Flexible Accelerated STOP Tetracycline Operator-Knockin (FAST): A Versatile and Efficient New Gene Modulating System. *Biol. Psychiatry* **67**, 770–773 (2010).

17. Skarnes, W. C. *et al.* A conditional knockout resource for the genome-wide study of mouse gene function. *Nature* **474**, 337–344 (2011).

18. Hao, X. *et al.* SNX25 regulates TGF-β signaling by enhancing the receptor degradation. *Cell. Signal.* **23**, 935–946 (2011).

19. Lau, J. *et al.* Temporal control of gene deletion in sensory ganglia using a tamoxifen-inducible Advillin-Cre-ERT2 recombinase mouse. *Mol. Pain* **7**, 1–13 (2011).

20. Kiermayer, C., Conrad, M., Schneider, M., Schmidt, J. & Brielmeier, M. Optimization of spatiotemporal gene inactivation in mouse heart by oral application of tamoxifen citrate. *Genesis* **45**, 11–16 (2007).

21. Hoeffel, G. *et al.* Adult Langerhans cells derive predominantly from embryonic fetal liver monocytes with a minor contribution of yolk sac-derived macrophages. *J. Exp. Med.* **209**, 1167–1181 (2012).

22. Tamoutounour, S. *et al.* Origins and functional specialization of macrophages and of conventional and monocyte-derived dendritic cells in mouse skin. *Immunity* **39**, 925–938 (2013).

23. Kierdorf, K., Katzmarski, N., Haas, C. A. & Prinz, M. Bone Marrow Cell Recruitment to the Brain in the Absence of Irradiation or Parabiosis Bias. *PLoS One* **8**, 1–10 (2013).

24. Ginhoux, F. *et al.* Fate mapping analysis reveals that adult microglia derive from primitive macrophages. *Science* **701**, 841–845 (2010).

25. Batlle, E. & Massagué, J. Transforming Growth Factor-β Signaling in Immunity and Cancer. *Immunity* **50**, 924–940 (2019).

26. Yona, S. *et al.* Fate Mapping Reveals Origins and Dynamics of Monocytes and Tissue Macrophages under Homeostasis. *Immunity* **38**, 79–91 (2013).

27. Madisen, L. *et al.* A toolbox of Cre-dependent optogenetic transgenic mice for light-induced activation and silencing. *Nat. Neurosci.* **15**, 793–802 (2012).

28. Fumagalli, S., Perego, C., Ortolano, F. & De Simoni, M. G. CX3CR1 deficiency induces an early protective inflammatory environment in ischemic mice. *Glia* **61**, 827–842 (2013).

29. Tsuda, M. *et al.* P2X4 receptors induced in spinal microglia gate tactile allodynia after nerve injury. *Nature* **424**, 778–783 (2003).

30. Hefti, F. F. *et al.* Novel class of pain drugs based on antagonism of NGF. *Trends Pharmacol. Sci.* **27**, 85–91 (2006).

31. Mantyh, P. W., Koltzenburg, M., Mendell, L. M., Tive, L. & Shelton, D. L. Antagonism of nerve growth factor-TrkA signaling and the relief of pain. *Anesthesiology* **115**, 189–204 (2011).

32. Chaumette, T. *et al.* c-Jun/p38MAPK/ASIC3 pathways specifically activated by nerve growth factor through TrkA are crucial for mechanical allodynia development. *Pain* **161**, 1109–1123 (2020).

33. Kensler, T. W., Wakabayashi, N. & Biswal, T. W. Cell survival responses to environmental stresses via the Keap1-Nrf2-ARE pathway. *Annu Rev Pharmacol Toxicol .* **47**, 89–116 (2007).

34. Shen, Z. *et al.* SNX16 activates c-Myc signaling by inhibiting ubiquitin-mediated proteasomal degradation of eEF1A2 in colorectal cancer development. *Mol. Oncol.* **14**, 387–406 (2020).

35. Tomlinson, R. E. *et al.* NGF-TrkA signaling in sensory nerves is required for skeletal adaptation to mechanical loads in mice. *Proc. Natl. Acad. Sci. U. S. A.* **114**, E3632–E3641 (2017).

36. Ding, J. *et al.* Macrophages are necessary for skin regeneration during tissue expansion. *J. Transl. Med.* **17**, 1–10 (2019).

37. Yu, X. *et al.* Dorsal root ganglion macrophages contribute to both the initiation and persistence of neuropathic pain. *Nat. Commun.* **11**, 1–12 (2020).

38. Grace, P., MR, H., Maier, S. & Watkins, L. Pathological pain and the neuroimmune interface. *Nat. Rev. Immunol.* **14**, 217–231 (2014).

39. Crawford, L. T. K. & Caterina, M. J. Functional Anatomy of the Sensory Nervous System: Updates From the Neuroscience Bench. *Toxicol. Pathol.* **48**, 174–189 (2020).

40. Ren, K. & Dubner, R. Interactions between the immune and nervous systems in pain. *Nat. Med.* **16**, 1267–1276 (2010).

41. van den Dries, K., Linder, S., Maridonneau-Parini, I. & Poincloux, R. Probing the mechanical landscape – new insights into podosome architecture and mechanics. *J. Cell Sci.* **132**, (2019).

42. Alonso, F., Spuul, P., Daubon, T., Kramer, Ij. & Génot, E. Variations on the theme of podosomes: A matter of context. *Biochim. Biophys. Acta - Mol. Cell Res.* **1866**, 545–553 (2019).

43. Paixão, S. *et al.* Identification of Spinal Neurons Contributing to the Dorsal Column Projection Mediating Fine Touch and Corrective Motor Movements. *Neuron* **104**, 749-764.e6 (2019).

44. Zimmerman, A. L. *et al.* Distinct Modes of Presynaptic Inhibition of Cutaneous Afferents and Their Functions in Behavior. *Neuron* **102**, 420-434.e8 (2019).

45. Wang, P. *et al.* SNX17 Recruits USP9X to Antagonize MIB1-Mediated Ubiquitination and Degradation of PCM1 during Serum-Starvation-Induced Ciliogenesis. *Cells* **8**, 1–19 (2019).

46. Nishimura, K., Tanaka, T., Takemura, S., Tatsumi, K. & Wanaka, A. SNX25 regulates proinflammatory cytokine expression via the NF-?B signal in macrophages. *PLoS One* **16**, 1–13 (2021).

47. Rysä, J., Tokola, H. & Ruskoaho, H. Mechanical stretch induced transcriptomic profiles in cardiac myocytes. *Sci. Rep.* **8**, 1–14 (2018).

48. Luo, X. *et al.* IL-23/IL-17A/TRPV1 axis produces mechanical pain via macrophage-sensory neuron crosstalk in female mice. *Neuron* 1–16 (2021). doi:10.1016/j.neuron.2021.06.015

49. Axelsson, H. E. *et al.* Transient receptor potential vanilloid 1, vanilloid 2 and melastatin 8 immunoreactive nerve fibers in human skin from individuals with and without Norrbottnian congenital insensitivity to pain. *Neuroscience* **162**, 1322–1332 (2009).

50. Wild, K. D. *et al.* Antibodies to nerve growth factor reverse established tactile allodynia in rodent models of neuropathic pain without tolerance. *J. Pharmacol. Exp. Ther.* **322**, 282–287 (2007).

51. Hefti, F. Pharmacology of nerve growth factor and discovery of tanezumab, an anti-nerve growth factor antibody and pain therapeutic. *Pharmacol. Res.* **154**, 104240 (2020).

52. Woolf, C. J., Safieh-Garabedian, B., Ma, Q. P., Crilly, P. & Winter, J. Nerve growth factor contributes to the generation of inflammatory sensory hypersensitivity. *Neuroscience* **62**, 327–331 (1994).

53. Tron, V. A., Coughlin, M. D., Jang, D. E., Stanisz, J. & Sauder, D. N. Expression and modulation of nerve growth factor in murine keratinocytes (PAM 212). *J. Clin. Invest.* **85**, 1085–1089 (1990).

54. Yamazaki, D. *et al.* The Mg2+ transporter CNNM4 regulates sperm Ca2+ homeostasis and is essential for reproduction. *J. Cell Sci.* **129**, 1940–1949 (2016).

55. Chaplan, S., Bach, F., Pogrel, J., Chung, J. & Yaksh, T. Quantitative assessment of tactile allodynia in the rat paw. *J Neurosci Methods .* **53**, 55–63 (1994).

Methods

Animals

Mlc1 TG mice (B6; CBB6(129)-Tg(Mlc1-tTA)2Rhn) were a gift from K.F. Tanaka (Keio University). *SNX25* constitutive KO (*Snx25* +/-) mice (B6/N-*Snx25*$^{tm1a/Nju}$, Nanjing BioMedical Research Institute of Nanjing University; strain name, B6/N-*Snx25*$^{tm1a/Nju}$, strain number, T001400) were obtained from Nanjing BioMedical Research Institute of Nanjing University (NBRI). *Snx25* cKO mice were generated by first crossing our *Snx25* LacZ/+ mice with CAG-Flpo mice (B6.Cg-Tg(CAG-FLPo)/1Osb), which were a gift from M. Ikawa (Osaka University), in order to excise the LacZ cassette framed by *Frt* sites and obtain an allele with floxed exon 4 (*Snx25*$^{loxP/loxP}$ mice)[54]. We crossed *Advillin*-cre mice (B6.Cg-Tg(*Avil-Cre*/ERT2)AJwo/J) (Jackson Laboratory, Stock No: 032027) with *Snx25*$^{loxP/loxP}$ mice to obtain *Avil*^{Cre}ERT2/WT; *Snx25*$^{loxP/loxP}$ mice. We crossed *Cx3cr1*^{Cre}ERT2 mice (B6.129P2(C)-*Cx3cr1*$^{tm2.1(Cre/ERT2)Jung/J}$) (Jackson Laboratory, Stock No: 020940) with *Snx25*$^{loxP/loxP}$ mice to obtain *Cx3cr1*^{Cre}ERT2/WT; *Snx25*$^{loxP/loxP}$ mice. We crossed *Cx3cr1*^{Cre}ERT2/WT; *Snx25*$^{loxP/loxP}$ mice with reporter mice RCL-eNpHR3.0-EYFP (Ai39 mice, Jackson Laboratory, Stock No: 014539) to obtain *Cx3cr1*^{Cre}ERT2/WT; *Snx25*$^{loxP/loxP}$; Ai39/+ mice. We crossed *Cx3cr1*^{Cre}ERT2/WT; *Snx25*$^{loxP/loxP}$ mice with reporter mice RCL-ChR2(H134R)/EYFP (Ai32 mice, Jackson Laboratory, Stock No: 024109) to obtain *Cx3cr1*^{Cre}ERT2/WT; *Snx25*$^{loxP/loxP}$; Ai32/+ mice. C57BL/6-Tg (CAG-EGFP) mice were purchased from Japan SLC (Hamamatsu, Japan). They were housed in standard cages under a 12 h light/dark cycle and temperature-controlled conditions. All the protocols for the animal experiments were approved by the Animal Care Committee of Nara Medical University in accordance with the policies established in the NIH Guide for the Care and Use of Laboratory Animals. This study was also carried out in compliance with the ARRIVE guidelines (https://arriveguidelines.org/).

Behavioral test

Paw mechanical sensitivity was assessed using von Frey's filaments based on the up-down method developed by Chaplan[55]. The von Frey's filaments used were: 0.07, 0.16, 0.4, 0.6, 1, 1.4, 2, 4 g. Animals were acclimatized for at least 15 min in individual clear acrylic cubicles (10 × 10 × 10 cm) placed on top of an elevated wire mesh. Quick withdrawal or licking of the paw after the 3 s stimulus was considered a positive response. Threshold values were derived according to the method described by Chaplan[55]. For the formalin test, 10 µl of 5% formalin was injected subcutaneously into the plantar surface of the right hind paw. PBS (10 µL) was injected into the plantar surface of the left hind paw. We calculated the durations of lifting, shaking, and licking of the formalin-injected paw. For hot plate test, mice were acclimatized for at least 2 h (1h/day x 2days) in individual clear acrylic cubicles placed on the preheated plate. The withdrawal latency in response to the stimulus was determined manually. To assess sensitivity to weak tactile stimulus, mice were acclimatized for at least 15 min in individual clear acrylic cubicles (10 × 10 × 10 cm) placed on top of an elevated wire mesh. Calibrated von Frey filaments (0.008-1g) were used to stimulate the plantar surface of the hind paws[43, 44]. Withdrawal following or immediately after the 1 s stimulus were considered as a positive response. Plantar surface was stimulated 10 times with each filament and the number of positive responses was measured[43, 44]. In all the behavioral tests, examiners were always blind to the genotypes of mice, the kinds of treatments, and the sides of hind

paws that received injections. After the evaluation was done, the behavioral data were analyzed by a different researcher.

Surgery of spared nerve injury (SNI) model

Surgical procedures were performed under 2% isoflurane anesthesia. SNI was made by a 6-0 polypropylene thread with tight ligation of the two branches of the right sciatic nerve, the common peroneal and the tibial nerves, followed by transection and removal of a 2-mm nerve portion. The sural nerve remained intact and any contact with or stretching of this nerve was carefully avoided. Muscle and skin were closed in two distinct layers.

Reagents

For tamoxifen (TAM) treatment, we employed oral administration. TAM (Sigma-Aldrich, St. Louis, MO, USA) was mixed with powdered chow (0.5 mg/g normal chow). This oral administration method is convenient for continuous administration and results in efficient induction of recombination while minimizing stress on the mice[20]. For *Snx25* deletion in BMDMs, we treated cells with *Snx25*-specific siRNA (Sigma Aldrich) using Lipofectamine RNAiMAX transfection reagent (Thermo Fisher). For *Snx25* deletion in BMDMs derived from *Cx3cr1*$^{Cre\text{ERT2/WT}}$; *Snx25*$^{loxP/loxP}$ mice, we treated cells with 1 mM 4-OH-tamoxifen (4-OHT, Sigma Aldrich) for 24 h. For inhibition of proteasomes, we used 5 mM MG132 (Sigma Aldrich) for 4 h. For depletion of macrophages in hind paw skin, we used clodronate liposome (MKV300, Cosmo Bio, Tokyo, Japan).

Clodronate liposome treatment

Twenty-microlitter of 10 mg/ml clodronate liposomes or control liposomes were subcutaneously injected into the right side of the hind paw skin on days 0 and 3. Skin sections were stained with anti-CD206 or anti-MHCII at day 6.

4-OHT treatment

For depletion of SNX25 in dermal macrophages, we administered 4-OHT (40 ng/mL, 10mL) by intradermal injection daily for seven days into *Cx3cr1*$^{Cre\text{ERT2/WT}}$; *Snx25*$^{loxP/loxP}$ mice or *Cx3cr1*$^{Cre\text{ERT2/WT}}$; *Snx25*$^{loxP/loxP}$; Ai32/+ mice. Vehicle was injected into the contralateral side of the same animal. At 8 days after the last injection, von Frey test was performed. Sections were stained with anti-GFP and anti-MHCII at day 11. For depletion of SNX25 in DRG, we administered 4-OHT (200 ng/mL, 20mL) into exposed DRG (L4) of *Cx3cr1*$^{Cre\text{ERT2/WT}}$; *Snx25*$^{loxP/loxP}$; Ai32/+ mice. At 5 days after administration, von Frey test was performed. DRG sections were stained with anti-GFP and anti-MHCII at day 5.

Immunohistochemistry

Mice were anesthetized and perfused transcardially with saline followed by 4% paraformaldehyde (PFA) in 0.1 M phosphate buffer (pH 7.4) (PB). Skin, DRG, sciatice nerve and spinal cord were removed,

postfixed overnight in the same fixative, and then immersed in 30% sucrose in PB overnight. Next, the tissues were frozen in powdered dry ice, embedded in Tissue-Tek OCT compound (Sakura Finetek, Torrance, CA), and stored at -80°C prior to sectioning. Eighteen-micrometer-thick sections were immersed in PBS containing 5% bovine serum albumin and 0.3% Triton X-100 for 1 h. Antibodies against mouse anti-CGRP (1:500, ab1887, abcam, Cambridge, UK), rabbit anti-c-Fos (1:10000, 226003, Synaptic Systems, Gottingen, Germany), rabbit anti-TRPV1 (1:100, KM018, Trans Genic, Fukuoka, Japan), rabbit anti-TrkA (1:150, ab76291, abcam), mouse anti-NF200 (1:1000, N0142, Sigma-Aldrich), mouse anti-PGP9.5 (1:500, ab8189, abcam), rat anti-MHCII (1:100, NBP1-43312, Novus Biologicals, Centennial, CO, USA), goat anti-CD206 (1:500, AF2535, R&D Systems, Minneapolis, MN, USA), rabbit anti-Iba1 (1:500, 019-19741, Wako, Osaka, Japan), rabbit anti-NGF (1:1000, sc-548, Santa Cruz Biotechnology, Santa Cruz, CA, USA), rat anti-GFP (1:5000, 04404-84, nacalai tesque, Kyoto, Japan), rabbit anti-GFP (1:5000, A6455, Thermo Fisher Scientific, Waltham, MA, USA), rabbit anti-SNX25 (1:500, 13294-1-AP, Proteintech, Rosemont, IL, USA), biotin mouse anti-CD4 (1:200, 100403, BioLegend, San Diego, CA), biotin mouse anti-CD8a (1:200, 100703, BioLegend), biotin mouse anti-Gr1 (1:200, 108403, BioLegend), biotin mouse anti-NK1.1 (1:200, 108703, BioLegend), biotin mouse anti-CD19 (1:200, 13-0193-81, eBioscience San Diego, CA), were applied overnight at 4°C. Alexa Fluor 488- and 594- (1:1000, Life Technologies, Grand Island, NY, USA) conjugated IgG were used as secondary antibodies. Sections were subjected to fluorescent Nissl staining (Neurotrace, Molecular Probes, Eugene, OR, USA). Images were captured using a confocal laser scanning microscope (C2, Nikon, Tokyo, Japan). For 3,3’-diaminozidine (DAB) staining, 8 mm-thick sections were immersed in PBS containing 5% bovine serum albumin and 0.3% Triton X-100 for 1 h. Antibodies against mouse anti-PGP9.5 (1:500, ab8189, abcam) were applied overnight at 4°C. After immunoreaction with DAB containing 0.03% H_2O_2 solution, sections were enclosed with mounting medium.

Microarray

Total RNA was isolated from the bone marrow of C57BL/6 mice and *Mlc1* TG mice using the NucleoSpin RNA Kit (Macherey-Nagel, Düren, Germany). The RNA samples were analyzed with Affymetrix GeneChip mouse genome 430 2.0 Arrays by Takara Bio (Otsu, Shiga, Japan).

Next-generation sequencing (NGS)

Whole-genome DNA was isolated from *Mlc1* TG mice using the NucleoBond AXG Column (Macherey-Nagel). Identification of the loci of transgene insertion was performed by Takara Bio, followed by NGS on the Illumina sequencing platform.

qRT-PCR

Total RNA of cells or tissues was extracted using a NucleoSpin RNA kit (Macherey-Nagel). Total RNA extracts were reverse-transcribed using random primers and a QuantiTect Reverse Transcription kit (QIAGEN, Hilden, Germany), according to the manufacturer’s instructions. Real-time PCR was performed using a LightCycler Quick System 350S (Roche Diagnostics), with THUNDERBIRD SYBR qPCR Mix (Toyobo, Osaka, Japan). PCR primers used in this study were as follows: *β-actin* sense primer, 5¢-

AGCCATGTACGTAGCCATCC-3¢; *β-actin* antisense primer, 5′-CTCTCAGCTGTGGTGGTGAA-3′; *Mlc1* sense primer, 5′-CTGACTCAAAGCCCAAGGAC-3′; *Mlc1* antisense primer, 5′-AGCGCAAATAATCCATCTCG-3′; *Mov10l1* sense primer, 5′-TGCTTCTGAACGTGGGACAGG-3′; *Mov10l1* antisense primer, 5′-ACACAGCCAATCAGCACTCTGG-3′; *Ngf* sense primer, 5′-TCAGCATTCCCTTGACACAG-3′; *Ngf* antisense primer, 5′-GTCTGAAGAGGTGGGTGGAG-3′; *Nrf2* sense primer, 5′-GCAACTCCAGAAGGAACAGG-3′; *Nrf2* antisense primer, 5′-GGAATGTCTCTGCCAAAAGC-3′; *Scn9a* sense primer, 5′-AAGGTCCCAAGCCCAGTAGT-3′; *Scn9a* antisense primer, 5′-AGGACTGAAGGGAGACAGCA-3′; *Scn10a* sense primer, 5′-GCCTCAGTTGGACTTGAAGG-3′; *Scn10a*, antisense primer, 5′-AGGGACTGAAGAGCCACAGA-3′; *Trpv1* sense primer, 5′-CCCTCCAGACAGAGACCCTA-3′; *Trpv1* antisense primer, 5′-GACAACAGAGCTGACGGTGA-3′.

Western blotting

Samples (cells or tissues) were lysed with 10 mM Tris, pH 7.4, containing 150 mM NaCl, 5 mM EDTA, 1% Triton X-100, 1% deoxycholic acid, and 0.1% sodium dodecyl sulfate (SDS). The homogenate was centrifuged at 20,600 *g* for 5 min, and the supernatant was stored at -20°C. Protein concentration was measured using a bicinchoninic acid protein assay kit (Pierce). Equal amounts of protein per lane were electrophoresed on SDS-polyacrylamide gels, and then transferred to a polyvinylidene difluoride membrane. The blots were probed with rabbit anti-SNX25 (1:1000, 13294-1-AP, Proteintech), rabbit anti-TRPV1 (1:100, KM018, Trans Genic), rabbit anti-TrkA (1:10000, ab76291, abcam), goat anti-CD206 (1:1000, AF2535, R&D Systems), rabbit anti-NGF (1:200, sc-548, Santa Cruz Biotechnology), rabbit anti-Nrf2 (1:500, sc-722, Santa Cruz Biotechnology), rabbit anti-HO-1 (1:500, ADI-SPA-896, Enzo Life Sciences, Farmingdale, NY, USA), rabbit anti-TGFbRI (1:200, sc-398, Santa Cruz Biotechnology) and rabbit anti-GAPDH (1:2000, ABS16, Burlington, MA, USA) antibodies. Immunoblot analysis was performed with horseradish peroxidase-conjugated anti-mouse and anti-rabbit IgG using enhanced chemiluminescence Western blotting detection reagents (Wako). Data were acquired in arbitrary densitometric units using Scion image software.

Co-immunoprecipitation

Cells were lysed with 50 mM Tris, pH 7.4, containing 150 mM NaCl, 1% NP-40, 0.5% deoxycholic acid, and protease inhibitor cocktail (Nacalai Tesque, Kyoto, Japan), and then incubated 4°C for 20 min with rotation. The lysate was centrifuged at 21,500 *g* for 15 min and the supernatant was collected. A rabbit IgG against Nrf2 (sc-722, Santa Cruz Biotechnology) was incubated with SureBeads Protein G Magnetic Beads (Bio-Rad, Berkeley, CA) for 10 min. The mixture was added to the supernatant for immunoprecipitation, incubated for 1 h with rotation, and then the immunobound protein was eluted.

Primary DRG neurons

DRGs from *Snx25* +/- and WT littermate mice were quickly collected in DMEM/F12 medium and incubated for 90 min at 37°C in a 0.2% collagenase solution. After dissociation, DRGs were transferred to a tube containing DMEM/F12 supplemented with 10% fetal bovine serum (FBS), 1%

penicillin/streptomycin solution. Ganglia were gently triturated using pipettes. After centrifugation, cells were resuspended in DMEM/F12 supplemented as above and plated on poly-L-lysine-coated culture dishes. Neurons were kept at 37°C in 5% CO_2 and the medium was changed to DMEM/F12 with B27 supplement 8 h after plating.

Fluo-4 Calcium assay

DRG neurons were seeded in 96-well cell culture plates at a density of 1.5×10^4 cells per well and cultured overnight. Intracellular calcium responses to capsaicin were measured using Calcium kit II-Fluo4 (CS32, Dojindo, Kumamoto, Japan) in accordance with the manufacturer's instructions. The temperature of the platform was controlled to 37°C. Cells were fluorescently imaged at 495-nm excitation every 7 s, and the fluorescence intensities of neurons were quantified at 515 nm. Fluorescence intensities of neurons were quantified simultaneously for the entire well. Capsaicin (10 mM) was added to measure the response.

Bone marrow transplantation (BMT)

BM recipients were male 8-week-old C57BL/6J, *Snx25* +/+, *Snx25* +/-, or $Snx25^{loxP/loxP}$ mice. Mice were intraperitoneally injected with the chemotherapeutic agent busulfan (30 μg/g body weight; B2635, Sigma-Aldrich) in a 1:4 solution of dimethyl sulfoxide and PBS 7, 5, and 3 days prior to bone marrow transfer. All mice were treated with antibiotics (trimethoprim/sulfamethoxazole) for 14 days after busulfan treatment. Bone marrow-derived cells were obtained from the femur and tibia of 5-week-old C57BL/6-Tg (CAG-EGFP), *Snx25* +/+, *Snx25* +/-, or $Cx3cr1^{Cre\text{ERT2/WT}}$; $Snx25^{loxP/loxP}$ mice and resuspended in PBS with 2% FBS. Bone marrow-derived cells (1×10^6) were transferred to 8-week-old male C57BL/6, *Snx25* +/+, *Snx25* +/-, or $Snx25^{loxP/loxP}$ recipient mice by tail vein injection (100 μL). For quantitative analysis, engraftment was verified by determining the percentage of EGFP-expressing cells in the blood. We counted the numbers of $EGFP^+$ cells in peripheral blood by flow cytometry and confirmed efficient chimerism as demonstrated by the large proportions of circulating blood leukocytes expressing EGFP.

Bone marrow-derived macrophage (BMDM) culture and application of mechanical stretch

Bone marrow cells were obtained from femur and tibia of 8-week-old male C57BL/6, *Snx25* +/+, *Snx25* +/-, or $Cx3cr1^{Cre\text{ERT2/WT}}$; $Snx25^{loxP/loxP}$ mice and cultured in RPMI-1640 medium containing 10% FBS, 1% penicillin/streptomycin, and 0.01% macrophage colony stimulating factor (M-CSF). After 6 days, the BMDMs were transferred to 3.5-mm dishes in RPMI-1640 containing 10% FBS and 1% penicillin/streptomycin. After overnight incubation, qPCR or Western blot analysis of BMDMs was performed. For mechanical stretch experiment, BMDMs were seeded to stretch chamber (STB-CH-04, STREX, Osaka, Japan) coated with 0.05 mg/ ml fibronectin (Millipore, #FC010) and exposed to stretch up to 12.5 %. Un-stretch control BMDMs were treated equally without application of mechanical stretch.

PCR array

The mouse inflammatory response and autoimmunity RT^2 Profiler PCR Array kit (PAMM-077Z, Qiagen) in a 96-well format was used. This kit profiles the expression of 84 genes that encode inflammatory response, autoimmunity, and other genes related to inflammation. Hind paw skins were quickly dissected 3 d after formalin injection, frozen rapidly, and stored at −80°C until use. Total RNA was purified using the NucleoSpin RNA kit (Macherey-Nagel) in accordance with the manufacturer's instructions. cDNA was obtained from purified RNA using the RT^2 First Strand Kit (Qiagen) provided with the PCR Array kit. cDNA template mixed with PCR master mix was dispensed into each well and real-time PCR was performed. Three independent arrays (three animals) were performed.

Fluorescent in situ hybridization (FISH)

FISH was performed with a probe targeting *Cx3cr1* mRNA using the RNAscope Fluorescent multiplex reagent kit (Advanced Cell Diagnostics, Hayward, CA, USA) according to the manufacturer's instructions.

Nerve ligation assay

To assess NGF/TrkA complex trafficking from the periphery toward the DRG cell bodies, we carefully exposed the left sciatic nerve and tightly ligated the nerve with one 6.0 suture in WT and *Snx25* +/- mice. Eight hours after the surgery, mice were terminally anesthetized and quickly perfused with 4% PFA. After perfusion, the left sciatic nerve was excised, post-fixed for 24 h in the same perfusion fixative, cryoprotected in 30% sucrose for 48 h at 4°C, and then frozen in tissue freezing medium (O.C.T.). Longitudinal sections (18 μm) of the left sciatic nerve were cut on a cryostat and then stored at -30°C before staining. Sciatic nerve sections were stained with the primary antibody against rabbit anti-TrkA (1:150, ab76291, abcam). Alexa Fluor 594- (Life Technologies) conjugated IgG was used as the secondary antibody.

Generation of constructs and transient transfection of 293T cells

PCR cloning was performed to amplify *Snx25* and *Nrf2* cDNA with a primer having an optimal Kozak consensus sequence just before the in-frame first ATG of the mouse *Snx25* and *Nrf2* genes. Fragments were inserted into the pcDNA3.1/Myc-His vector (Invitrogen). Using the LipofectAMINE reagent (Invitrogen), 293T cells were transfected with a *Snx25* and *Nrf2* construct according to the manufacturer's instructions.

Fluorescence activated cell sorting (FACS)

Hind paw skin from *Cx3cr1*^{Cre}ERT2/WT; *Snx25*$^{loxP/loxP}$ mice (±TAM) were collected and dissociated using Multi Tissue Dissociation Kit 1 (Miltenyi Biotec, Germany). After dissociation, the cells were stained with various combinations of mAbs. The mAbs used in this study were Alexa Fluor 488–anti-CD11b (1:100, Biolegend, San Diego, CA), Alexa Fluor 647-anti-F4/80 (1:100, Biolegend), PE/Cyanine7 anti-CD45 (1:100, Biolegend). After washing, the cells were stained with 7-AAD (BD Biosciences) to exclude the dead cells

from analysis. Macrophages (CD45+ CD11bhigh F4/80high) from the hind paw skin were isolated by the FACSAria (> 96% purity).

Quantification and statistical analysis

Quantifications were performed from at least three independent experimental groups. Data are presented as mean ± SEM. Statistical analyses were performed using Student's *t*-test or Welch's *t*-test for two groups or one-way ANOVA for multiple groups, and significant differences between group means were identified with the Tukey–Kramer test. Statistical significance is indicated as asterisks. *$p < 0.05$, **$p < 0.01$. All n are indicated in Figure legends.

Figures

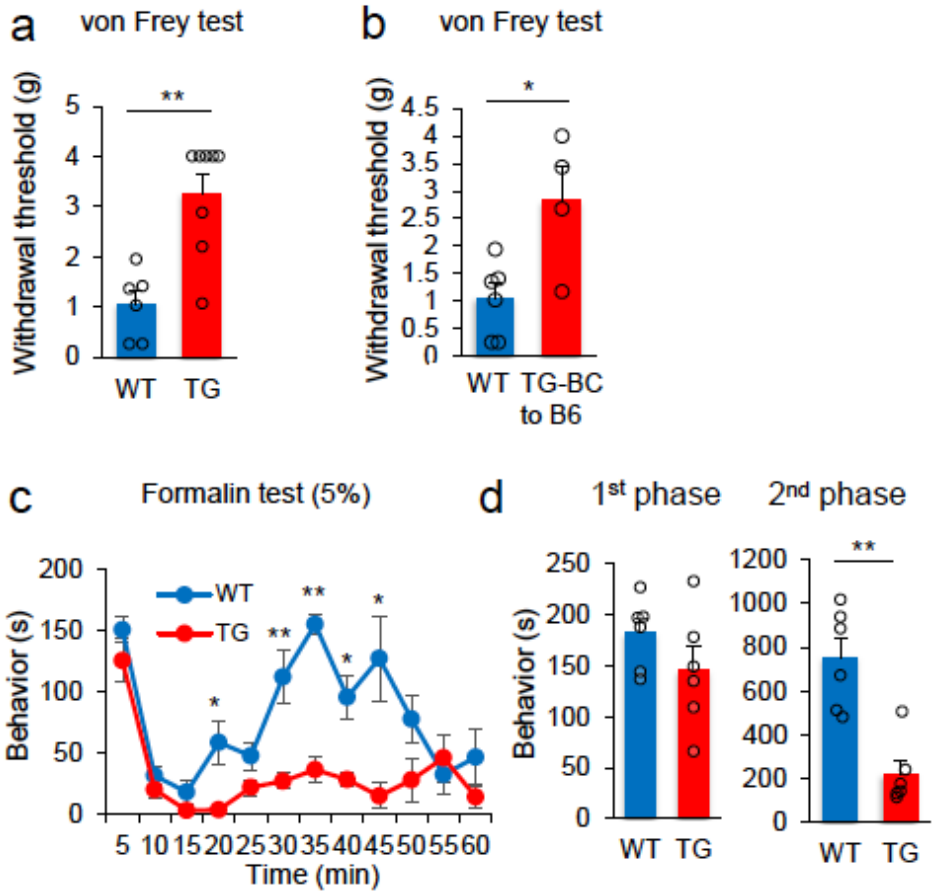

Fig. 1 Tanaka *et al.*

Figure 1

Mlc1 TG mice show a pain-insensitive phenotype. (a) Comparison of paw withdrawal thresholds to mechanical stimulation with von Frey filaments between wild type (WT; n = 6) and Mlc1 TG mice (TG; n = 8). (b) The same von Frey test except that Mlc1 TG mice (mixed 129S6/CBA/C57BL/6J background) were backcrossed with C57BL/6J mice for 7 generations (WT: n = 6; Mlc-1 TG-BC to B6: n = 4). (c) Formalin test of wild type and Mlc1 TG mice. Pain-related behavior time including licking, lifting, and

flinching of the 5% formalin-injected paw was plotted for 5-minute periods (WT: n = 6; TG: n = 6). (d) Left, measurement of the behavior time in 1st phase (0–10 min). Right, measurement of the behavior time in 2nd phase (20–60 min). Results are represented as mean ± SEM of 3–5 independent experiments. Statistical significance was calculated using the Student's t-test. *p < 0.05, **p < 0.01.

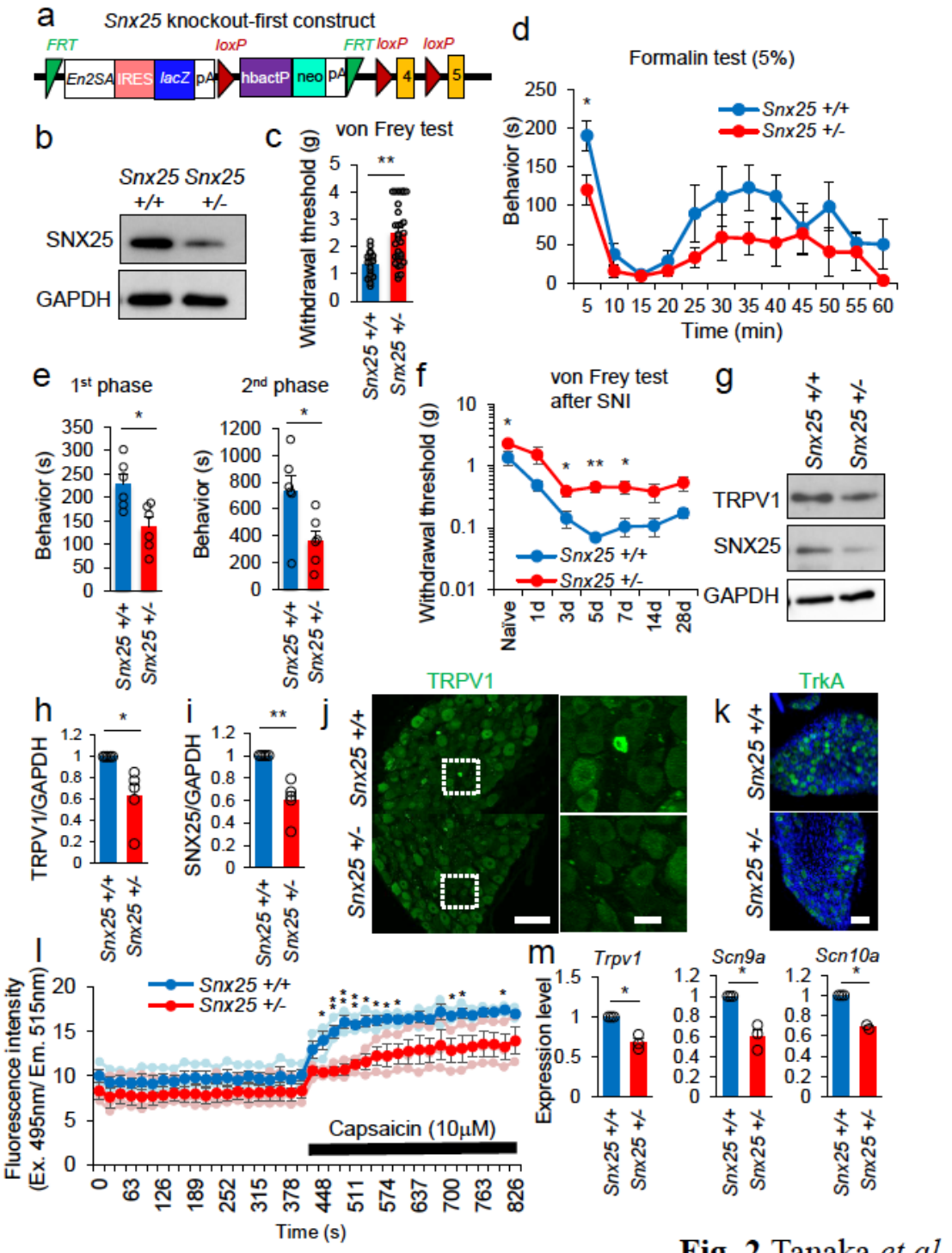

Fig. 2 Tanaka *et al.*

Figure 2

Snx25 +/- mice show a pain-insensitive phenotype. (a) Scheme of the targeting vector used to knock out the Snx25 gene. (b) Expression level of SNX25 in the lung of WT and Snx25 +/- mice. (c) von Frey test showing significant elevation of withdrawal thresholds in heterozygotes relative to WT mice. (WT: n = 16; Snx25 +/-: n = 28). (d-e) Formalin test of WT and Snx25 +/- mice. Pain-related behavior time including licking, lifting, and flinching of the formalin (5%)-injected paw was plotted for 5-minute periods (WT: n = 6; Snx25 +/-: n = 6). (e) Left panel shows total pain-related behavior time in 1st phase (0–10 min). Right panel indicates 2nd phase (20–60 min). (f) Mechanical allodynia was evaluated by von Frey test after spared nerve injury (SNI) in mice (WT: n = 4; Snx25 +/-: n = 7). Snx25 +/- mice showed dull responses to von Frey filaments as compared to the WT mice. (g) Representative Western blots show expression levels of TRPV1 and SNX25 in the DRG of WT and Snx25 +/- mice. (h and i) Semi-quantitative analyses of Western blotting data (WT: n = 5; Snx25 +/-: n = 5). (j) Confocal images of the DRG stained with anti-TRPV1 antibody in WT and Snx25 +/- mice. Scale bar, 100 μm. Right panels show magnified views of boxed areas in the corresponding left panels. Scale bar, 20 μm. (k) Confocal images of the DRG of WT and Snx25 +/- mice, stained with anti-TrkA antibody. Scale bar, 100 μm. (l) Fluo-4 Ca imaging of primary DRG neurons from an entire well dissociated from WT and Snx25 +/- mice (WT: n = 3; Snx25 +/-: n = 3). (m) mRNA expression levels for pain-related factors in DRG of Snx25 +/- mice were significantly lower than those of WT mice (WT: n = 3; Snx25 +/-: n = 3). Results are represented as mean ± SEM of 3–5 independent experiments. Significance was calculated using the Student’s t-test (c, d, e and f) or Welch’s t-test (h, i and m). *$p < 0.05$, **$p < 0.01$.

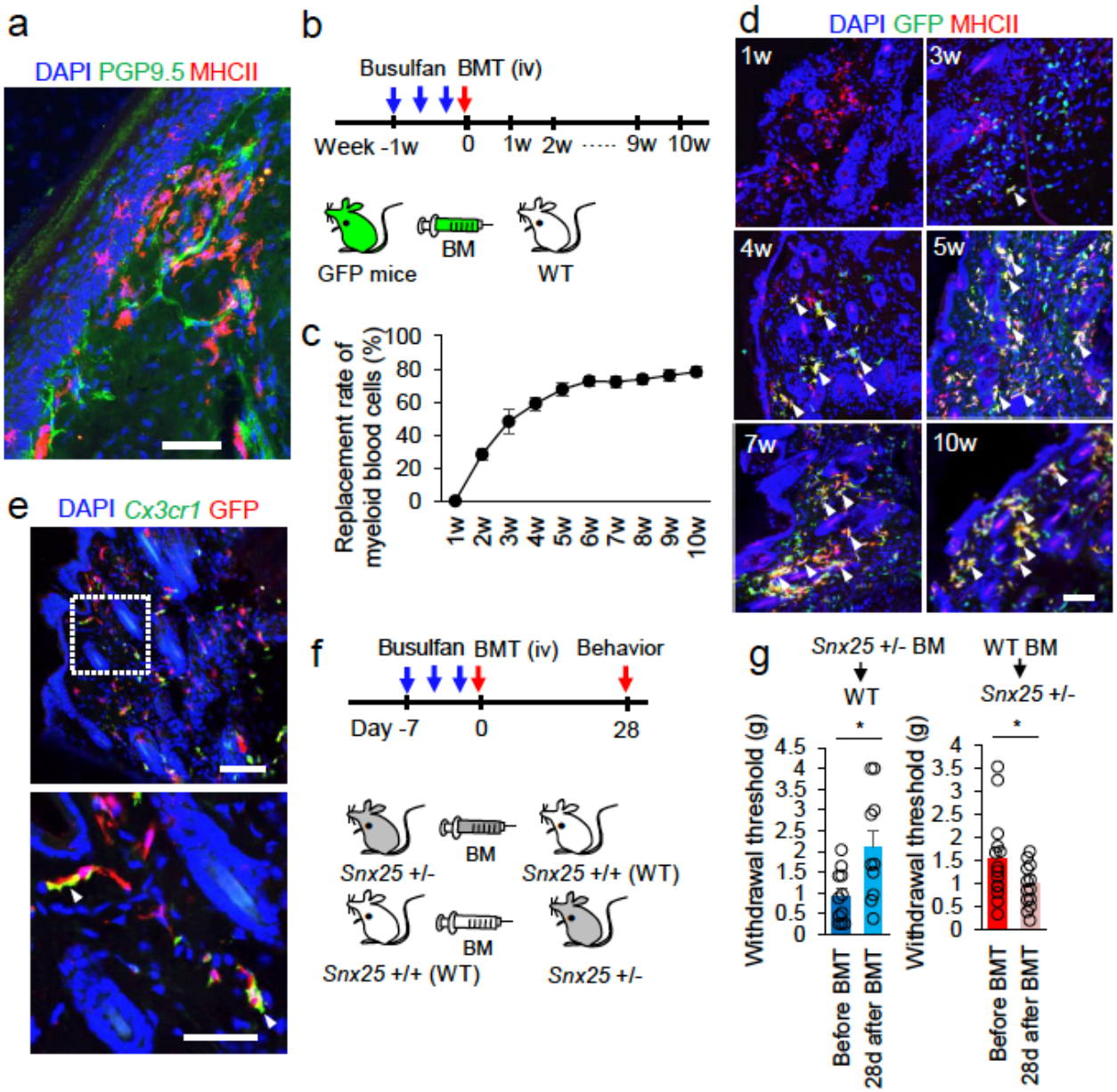

Fig. 3 Tanaka *et al.*

Figure 3

SNX25 in macrophages derived from BM contribute to pain sensation. (a) Confocal images of the plantar skin of the hind paw (naive) of WT mice, immunolabeled for PGP9.5 and MHCII. Dermal macrophages are closely associated with PGP9.5-positive nerve. Scale bar, 50 μm. (b) Experimental schedule of bone marrow transplantation (BMT). BM chimeric mice were generated by transplanting BM of GFP mice (green mice) to WT mice (intravenous (iv) tail vein injection). (c) Chimerism of myeloid cells in peripheral

blood, plotted against time after transplantation. n = 4. (d) Confocal images of hind paw skin stained for GFP and MHCII in WT mice with BM of green mice. Arrowheads denote double-labeled cells. Scale bar, 100 μm. (e) Confocal images of hind paw skin stained for GFP (Alexa-594) and Cx3cr1 mRNA (FISH) in WT mice with BM of green mice (5w after transplantation). BM-derived cells are also positive for Cx3cr1 mRNA (arrowheads). Scale bar, 100 μm. The lower panel is a magnified view of the boxed area in the upper panel. Scale bar, 50 μm. (f) Experimental schedule of cross-transplantation of BMs between WT and Snx25 +/- mice and behavioral evaluation of chimeric mice. (g) Paw withdrawal thresholds to mechanical stimulation with von Frey filaments approached the levels of donors in both chimeras (Snx25 +/- BM → WT: n = 10; WT BM → Snx25 +/-: n = 13) compared to thresholds before BMT. Results are represented as mean ± SEM of 3 independent experiments. Significance was calculated using the Student's t-test. *p < 0.05.

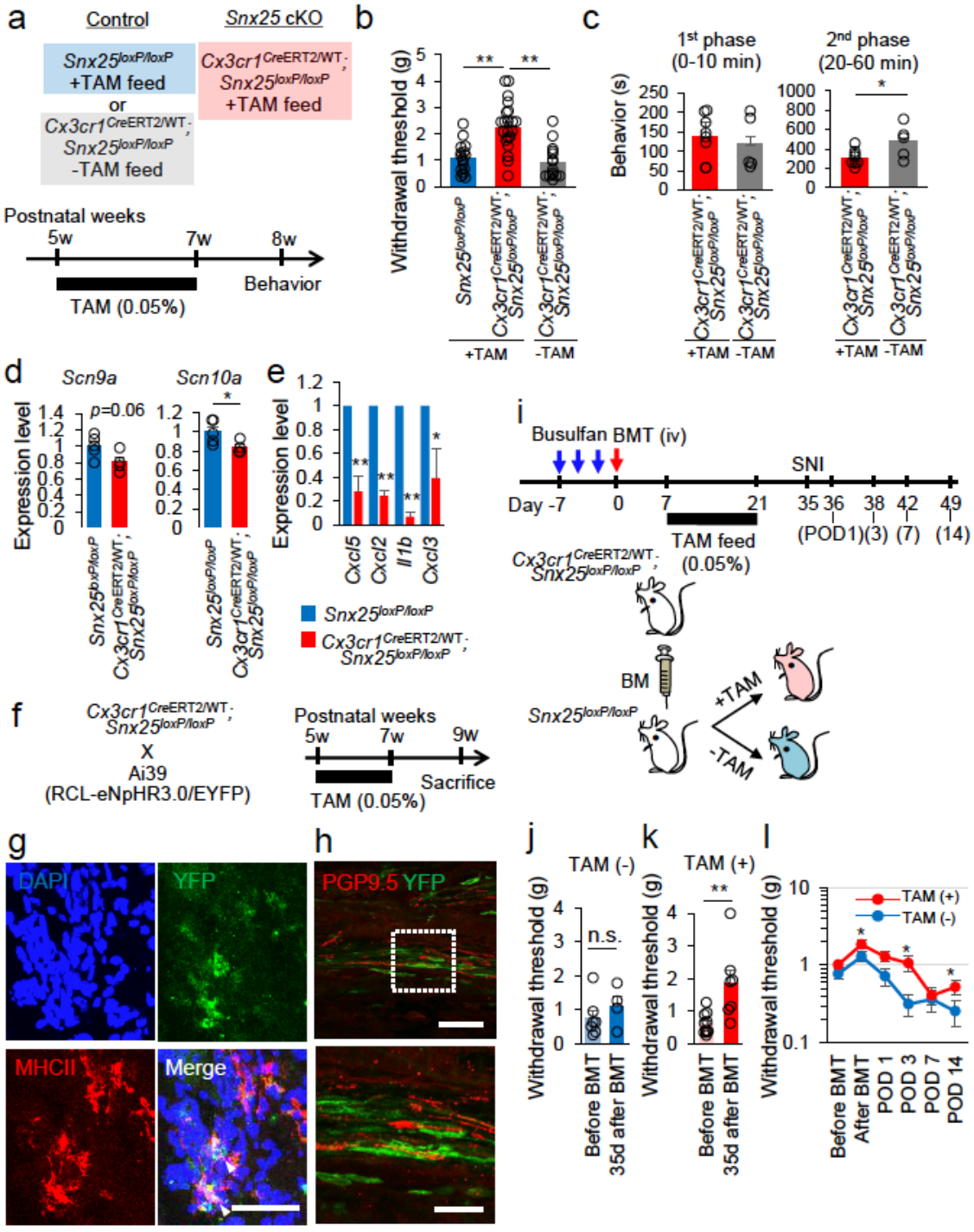

Fig. 4 Tanaka *et al.*

Figure 4

Snx25 conditional KO in macrophages renders a pain-insensitive phenotype. (a) Experimental schedule of conditional KO generation and behavioral analyses. (b) Conditional KO mice (tamoxifen (TAM)-treated Cx3cr1CreERT2/WT; Snx25loxP/loxP mice) exhibited significantly higher thresholds than the controls without tamoxifen treatment or than the floxed mice without the Cre driver (Snx25loxP/loxP mice (+ TAM): n = 17; Cx3cr1CreERT2/WT; Snx25loxP/loxP mice (+ TAM): n = 25; Cx3cr1CreERT2/WT;

Snx25loxP/loxP mice (- TAM): n = 14). (c) Formalin tests showed that the pain-related behavior time of conditional KO mice was significantly shorter than the control without tamoxifen treatment only in the 2nd phase. (Cx3cr1CreERT2/WT; Snx25loxP/loxP mice +TAM: n = 8; -TAM: n = 5). (d) Conditional KO DRGs had lower Na channel mRNAs than the control DRGs. (e) Chemokines and cytokines were significantly downregulated in the conditional KO skin as compared to the control. (f) Experimental schedule of the visualization of conditional KO cells in the dermis. (g) Confocal images of hind paw skin (naive) stained for YFP (green) and MHCII in Cx3cr1CreERT2/WT; Snx25loxP/loxP; Ai39/+ mice. Arrowheads denote double-labeled cells. Scale bar, 50 μm. (h) Confocal images of hind paw skin stained for YFP (green) and PGP9.5 in Cx3cr1CreERT2/WT; Snx25loxP/loxP; Ai39/+ mice. Scale bar, 50 μm. The lower panel is a magnified view of the boxed area. Scale bar, 20 μm. (i) Schedules for generation of BM chimeric mice by transplanting Cx3cr1CreERT2/WT; Snx25loxP/loxP BM into Snx25loxP/loxP mice and Cx3cr1CreERT2/WT; Snx25loxP/loxP mice, and subsequent spared nerve injury experiments. (j) Even at 35 days after BMT, mechanical pain sensing was comparable to that before BMT if we did not administer tamoxifen (-TAM). (k) The same experimental setting as (j) except that we treated BM chimeric mice with tamoxifen (+TAM), yielding a significant increase in withdrawal thresholds to von Frey mechanical stimulation relative to those before BMT. (l) Establishment and time course of mechanical allodynia were plotted after BMT and SNI in Snx25loxP/loxP (Cx3cr1-CreERT2/WT; Snx25loxP/loxP BM) mice (-TAM: n = 4; +TAM: n = 12). Results are represented as mean ± SEM of 3–5 independent experiments. Significance was calculated using one-way ANOVA (b) or the Student's t-test (c, d, j, k, and l) or Welch's t-test (e). *$p < 0.05$, **$p < 0.01$.

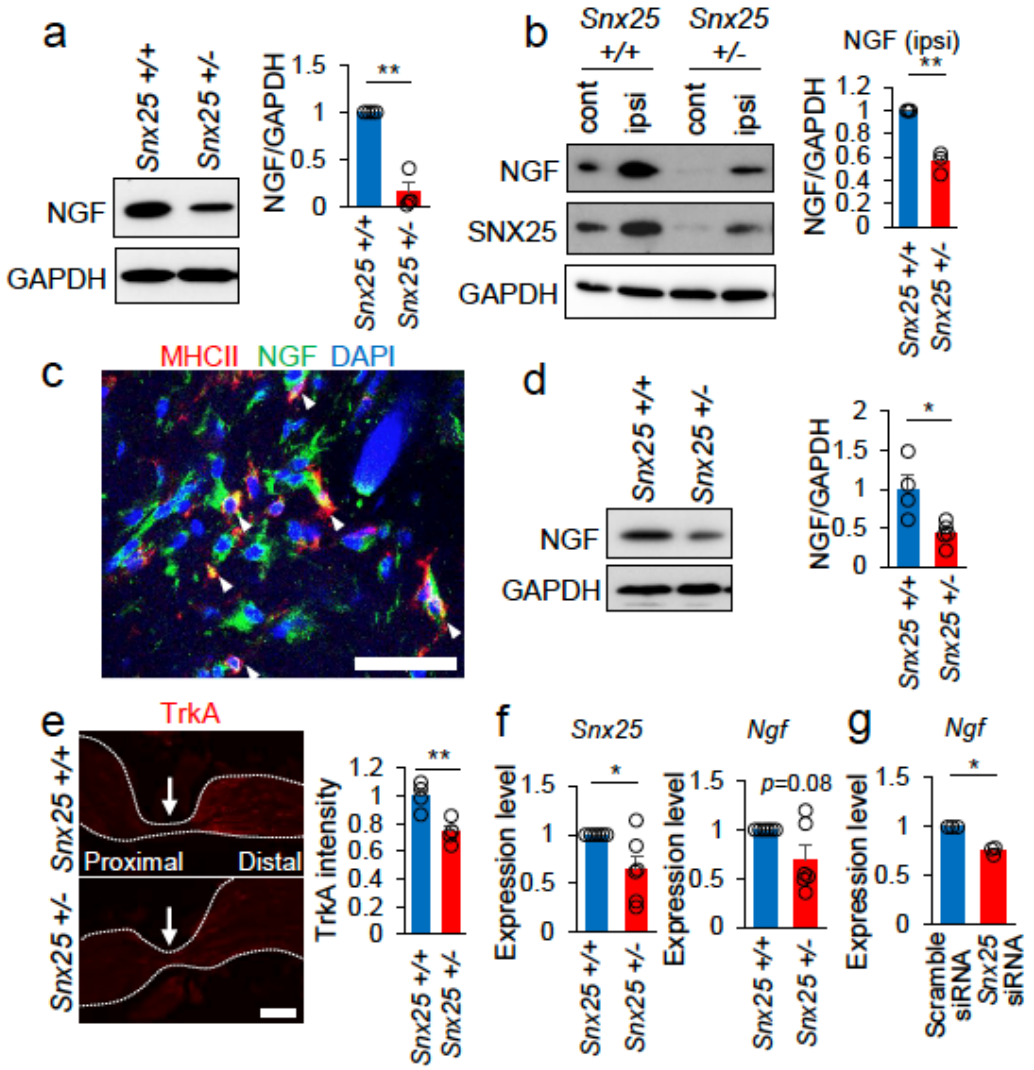

Fig. 5 Tanaka *et al.*

Figure 5

NGF expression in macrophages is reduced in Snx25 +/- mice. (a) A representative Western blot showing NGF levels in the hind paw skin of WT and Snx25 +/- mice. The graph shows semi-quantitative analyses. (b) Semi-quantitative analyses of NGF levels in the hind paw skin of WT and Snx25 +/- mice at 30 min after formalin injection. The graph shows that NGF levels in the ipsilateral side were significantly decreased in the heterozygote mice. (c) Confocal images of hind paw skin immunolabeled for NGF and

MHCII in WT mice. Arrowheads denote double-labeled cells. Scale bar, 50 μm. (d) Expression levels of NGF in BMDMs of WT and Snx25 +/- mice were examined by Western blotting, normalized with GAPDH content, and analyzed semi-quantitatively (WT: n = 4; Snx25 +/-: n = 5). (e) Left, confocal images of sciatic nerve sections immunolabeled for TrkA at 8 h after nerve ligation (arrows indicate ligation site) in WT and Snx25 +/- mice. Right, semi-quantitative analysis of the TrkA accumulation on the distal side of the nerve ligature. Scale bar, 200 μm. (f) Expression profiles of mRNAs for Snx25 and Ngf in BMDMs of WT and Snx25 +/- mice (WT: n = 6; Snx25 +/-: n = 6). (g) Ngf mRNA was quantified by RT-PCR in BMDMs transfected with either Snx25 siRNA or scramble siRNA (scramble siRNA: n = 3; Snx25 siRNA: n = 3). Results are represented as mean ± SEM of 3–5 independent experiments. Statistical analyses were performed using the Student's t-test (d and e) or Welch's t-test (a, b, f and g). *$p < 0.05$, **$p < 0.01$.

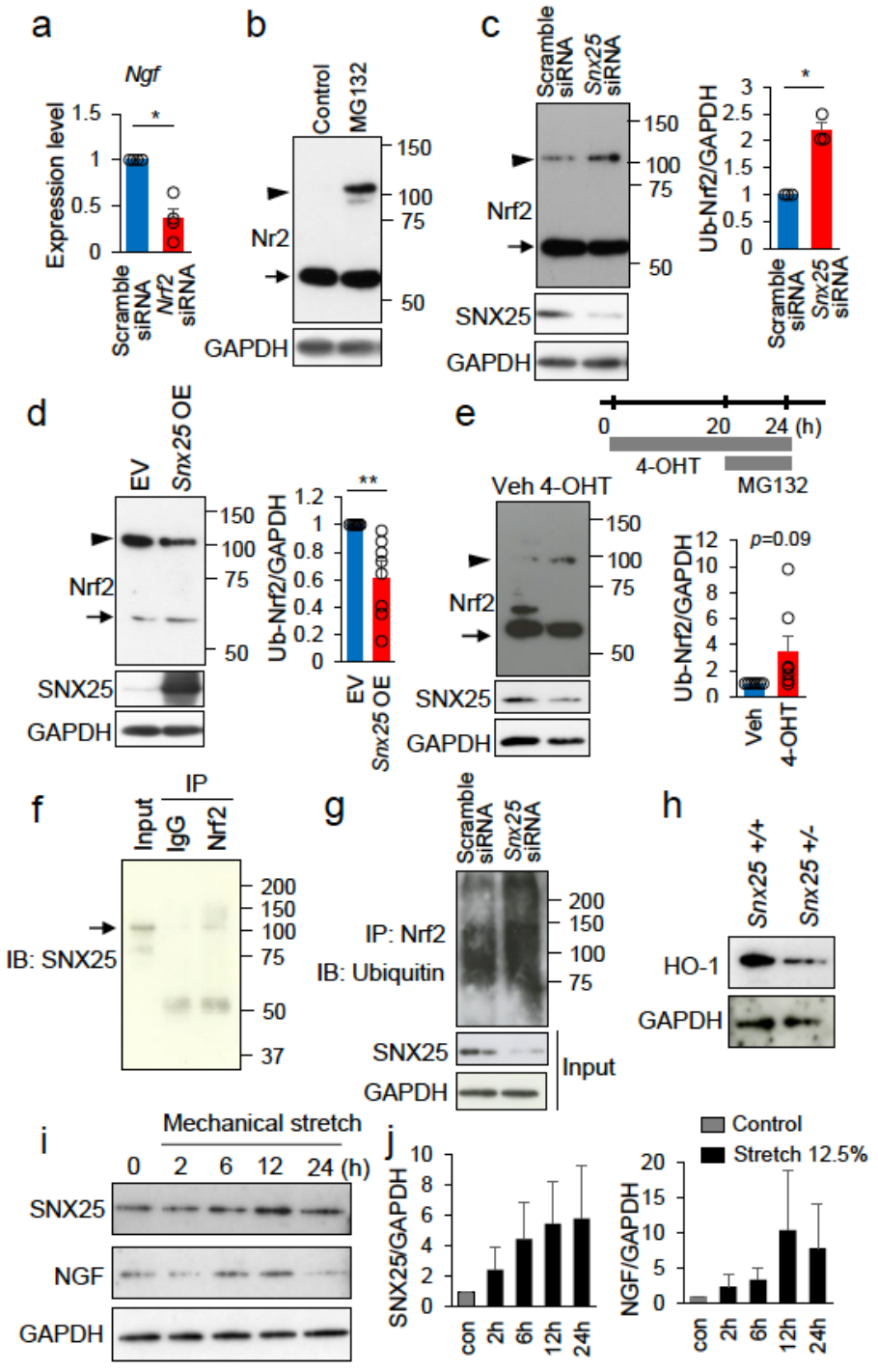

Fig. 6 Tanaka *et al.*

Figure 6

SNX25 activates Ngf production by inhibiting ubiquitin-mediated degradation of Nrf2. (a) Ngf mRNA levels in BMDMs transfected with either Nrf2 siRNA or scramble siRNA were analyzed semi-quantitatively by RT-PCR. (scramble siRNA: n = 4; Snx25 siRNA: n = 4). (b) A representative Western blot showing Nrf2 protein levels in BMDMs in the presence or absence of MG132. Arrow: Nrf2 (61–68 kDa); arrowhead: poly-ubiquitinated Nrf2 (100–110 kDa). (c) Ubiquitination levels of Nrf2 protein were probed in 293T cells

transfected with Snx25 siRNA or scramble siRNA in the presence of MG132 (scramble siRNA: n = 3; Snx25 siRNA: n = 3). Arrow: Nrf2; arrowhead: poly-ubiquitinated Nrf2. Semi-quantitative analysis revealed that the band intensity of poly-ubiquitinated Nrf2 (Ub-Nrf2) is significantly higher in the Snx25 knock-down cells than in the control. (d) Nrf2 and poly-ubiquitinated Nrf2 were probed in 293T transfected with full-length Snx25 expression vector (Snx25 OE) or empty vector (EV) in the presence of MG132 (empty vector + Nrf2 vector: n = 8; Snx25 vector + Nrf2 vector: n = 8). Arrow: Nrf2; arrowhead: poly-ubiquitinated Nrf2. Semi-quantitative analysis shows that the intensity of Ub-Nrf2 in the Snx25-overexpressing cells was significantly lower than that in the cells transfected with empty vector. (e) Nrf2 was examined by Western analyses in BMDMs of Cx3cr1CreERT2/WT; Snx25loxP/loxP treated with 4-OH-tamoxifen (4-OHT) or without 4-OHT (vehicle (Veh)) in the presence of MG132 (Veh: n = 7; 4-OHT: n = 7). Arrow: Nrf2; arrowhead: poly-ubiquitinated Nrf2. 4-OHT treatment significantly increased ubiquitinated species of Nrf2. (f) Co-immunoprecipitation (Co-IP) was performed in 293T cells expressing SNX25 and Nrf2. Cell lysates were immunoprecipitated with anti-Nrf2 antibody and immunoblotted with anti-SNX25 antibody. Normal IgG was used as negative control. Arrow: SNX25. (g) The level of ubiquitin-bound Nrf2. SNX25-knockdown BMDMs were treated with MG132, and cell lysates were immunoprecipitated with anti-Nrf2 antibody and immunoblotted with anti-ubiquitin antibody. (h) A representative Western blot of heme oxigenase-1 (HO-1), a stress-inducible and downstream gene of Nrf2 transcription factor, in the hind paw skin of WT and Snx25 +/- mice. (i-j) Semi-quantitative analyses of SNX25 and NGF levels in mechanically stretched BMDMs. BMDMs were exposed to mechanical stretch over time period of 24 h. Mechanical stretch to 12.5% of BMDMs increases SNX25 and NGF protein expression in a time dependent manner. Results are represented as mean ± SEM of 3–5 independent experiments. Statistical analyses were performed using the Welch's t-test. *$p < 0.05$, **$p < 0.01$.

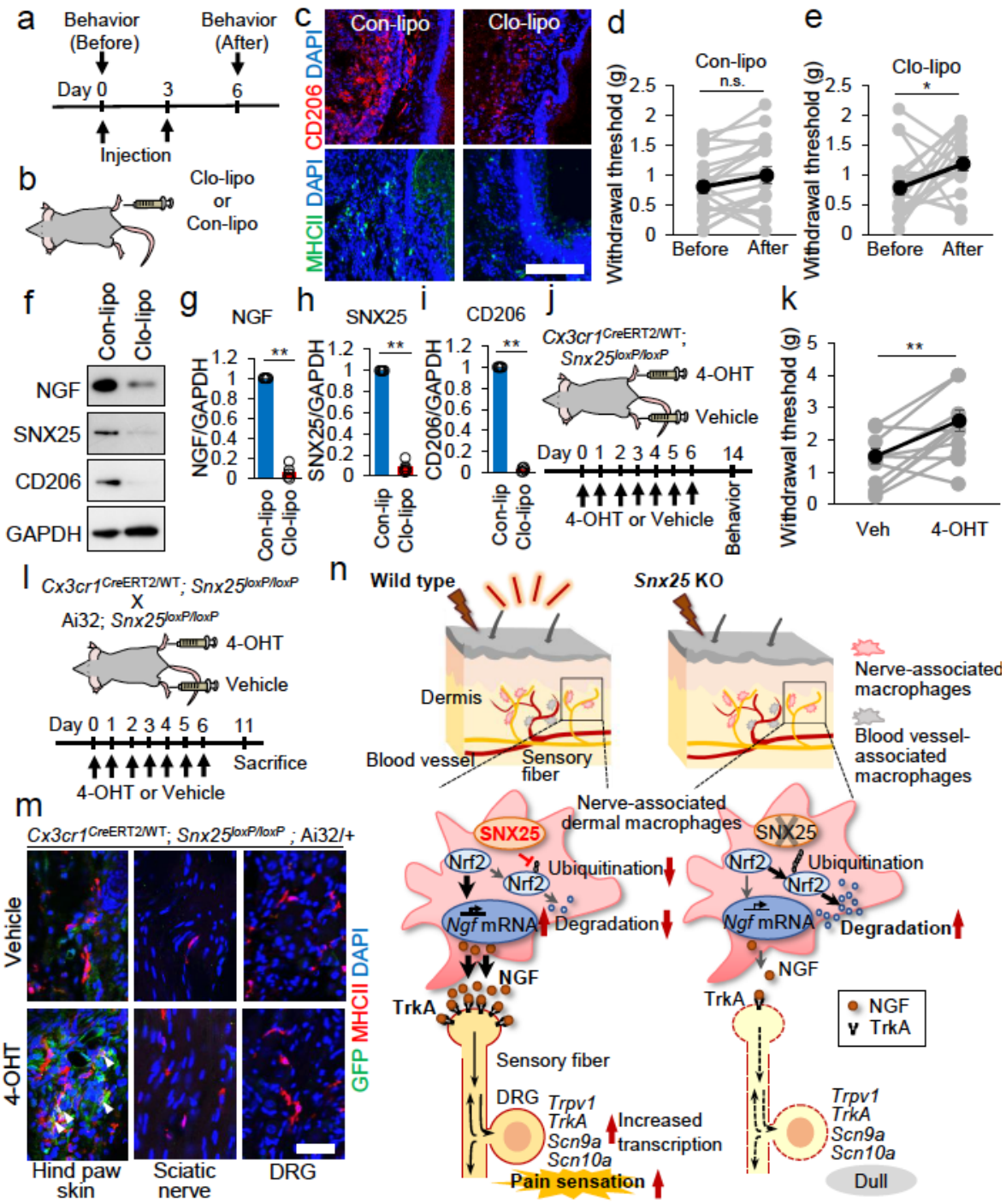

Fig. 7 Tanaka *et al.*

Figure 7

Dermal macrophages are sufficient to initiate pain sensation and SNX25 is a key factor in this process. (a) Experimental schedule of macrophage killing in the dermis. (b) Control liposomes (Con-lipo) and clodronate liposomes (Clo-lipo) were injected into hind paws. (c) Confocal images of hind paw skin immunolabeled for CD206 or MHCII in WT mice injected with Con-lipo or Clo-lipo. Scale bar, 200 μm. (d-e) Paw withdrawal thresholds to von Frey filaments on the Con-lipo-injected side (n = 20) or Clo-lipo-injected

side (n = 20). (f–i) Expression levels of NGF, SNX25 and CD206 in the hind paw skin of the Con-lipo-injected and Clo-lipo-injected sides were examined by Western blotting (f) and semi-quantitatively compared for NGF (g), SNX25 (h) and CD206 (i). n = 5. (j) Scheme depicting dermal injection of vehicle or 4-OHT into hind paws of a Cx3cr1CreERT2/WT; Snx25loxP/loxP mouse and experimental time course. To achieve gene recombination, we injected 4-OHT daily for 7 days and pain behavior was evaluated at 1 week after last injection. (k) Paw withdrawal thresholds to von Frey filaments are compared between the vehicle- and 4-OHT-injected sides (n = 11). (l) Scheme depicting dermal injection of vehicle or 4-OHT into hind paws of a Cx3cr1CreERT2/WT; Snx25loxP/loxP; Ai32/+ mouse and experimental time course. (m) Confocal images of hind paw skin, sciatic nerve, and DRG immunolabeled for MHCII or GFP injected with 4-OHT into dermis. Scale bar, 50 μm. Results are represented as mean ± SEM of 3-5 independent experiments. Statistical analyses were performed using the Student's t-test (d, e and k) or Welch's t-test (g-i). *p < 0.05, **p < 0.01. (n) Schematic representation of how SNX25 in dermal macrophages sets pain sensitivity via Nrf2–NGF/TrkA signaling and of how Snx25 KO results in a dull phenotype.

Supplementary Files

This is a list of supplementary files associated with this preprint. Click to download.

- Supplementaryinformation210902.docx